

Concordant Rb–Sr, Sm–Nd, and Ar–Ar ages for Northwest Africa 1460: A 346 Ma old basaltic shergottite related to “lherzolitic” shergottites

L.E. Nyquist^{a,*}, D.D. Bogard^a, C.-Y. Shih^b, J. Park^{a,c,1}, Y.D. Reese^d, A.J. Irving^e

^a *KRIARES NASA Johnson Space Center, Houston, TX 77058-3696, USA*

^b *JE23 Jacobs Technology, ESCG, Houston, TX 77258-8447, USA*

^c *NASA Postdoctoral Program, Oak Ridge Associated Universities, Oak Ridge, TN 37831-0117, USA*

^d *JE23 Muniz Engineering, ESCG, Houston, TX 77258-8447, USA*

^e *Dept. of Earth & Space Sciences, University of Washington, Seattle, WA 98195, USA*

Received 18 June 2008; accepted in revised form 15 April 2009; available online 24 April 2009

Abstract

Multiple lines of evidence show that the Rb–Sr, Sm–Nd, and Ar–Ar isotopic systems individually give robust crystallization ages for basaltic (or diabasic) shergottite Northwest Africa (NWA) 1460. In contrast to other shergottites, NWA 1460 exhibits minimal evidence of excess ^{40}Ar , thus allowing an unambiguous determination of its Ar–Ar age. The concordant Rb–Sr, Sm–Nd, and Ar–Ar results for NWA 1460 define its crystallization age to be 346 ± 17 Ma (2σ). In combination with petrographic and trace element data for this specimen and paired meteorite NWA 480, these results strongly refute the suggestion by others that the shergottites are ~ 4.1 Ga old. Current crystallization and cosmic-ray exposure (CRE) age data permit identification of a maximum of nine ejection events for Martian meteorites (numbering more than 50 unpaired specimens as of 2008) and plausibly as few as five such events. Although recent high resolution imaging of the Martian surface has identified limited areas of sparsely cratered terrains, the meteorite data suggest that either these areas are representative of larger areas from which the meteorites might come, or that the cratering chronology needs recalibration. Time-averaged $^{87}\text{Rb}/^{86}\text{Sr} = 0.16$ for the mantle source of the parent magma of NWA 1460/480 over the ~ 4.56 Ga age of the planet is consistent with previously estimated values for bulk silicate Mars in the range 0.13–0.16, and similar to values of ~ 0.18 for the “lherzolitic” shergottites. Initial ϵ_{Nd} for NWA 1460/480 at 350 ± 16 Ma ago was $+10.6 \pm 0.5$, which implies a time-averaged $^{147}\text{Sm}/^{144}\text{Nd}$ of 0.217 in the Martian mantle prior to mafic melt extraction, similar to values of 0.211–0.216 for the “lherzolitic” shergottites. These time-averaged values do not imply a simple two-stage mantle/melt evolution, but must result from multiple episodes of melt extractions from the source regions. Much higher “late-stage” ϵ_{Nd} values for the depleted shergottites imply similar processes carried to a greater degree. Thus, NWA 1460/480, the “lherzolitic” shergottites and perhaps EET 79001 give the best (albeit imperfect) estimate of the Sr- and Nd-isotopic characteristics of bulk silicate Mars.

Published by Elsevier Ltd.

1. INTRODUCTION

Northwest Africa 1460 is an extremely fresh, completely fusion-crusting Martian meteorite that was found in the Moroccan desert in 2001 (Connolly et al., 2006). This 70.2 g, relatively coarse grained basaltic (or more properly diabasic) shergottite is paired with a smaller but otherwise indistinguishable stone (Northwest Africa 480) found a

* Corresponding author. Fax: +1 281 483 5038.

E-mail address: laurence.e.nyquist@nasa.gov (L.E. Nyquist).

¹ Present address: Lunar and Planetary Institute, Houston, TX, 77058, USA.

year earlier near the same location by the same nomad (Barrat et al., 2002; Irving and Kuehner, 2003). Both specimens are composed mainly of pale yellowish-green prismatic grains of low-Ca pyroxenes (up to 5 mm long) with subordinate gray, glassy maskelynite laths (converted from plagioclase by shock) and accessory phases. Although both meteorites were found in a hot desert environment, they do not contain any calcite, sulfates or iron oxyhydroxides (Lorand et al., 2005), and judging from their glistening black fusion crusts must represent a very recent but unobserved fall of at least two stones. Because NWA 1460 lacks any petrographic evidence of secondary alteration mineralogy, it is particularly well suited for geochronological studies. We thus undertook a coordinated Rb–Sr/Sm–Nd/Ar–Ar isotopic study of this fresh igneous rock to (a) extend, if possible, the observed range of radiometric ages of Martian meteorites, and (b) investigate the isotopic systematics of a Martian meteorite that *a priori* should be free of isotopic perturbations resulting from any hypothesized interaction with Martian subsurface fluids (Bouvier et al., 2005, 2008).

Although NWA 480 and NWA 1460 are completely lacking in olivine, the bulk chemical composition (especially the rare earth element pattern) of NWA 480 led Barrat et al. (2002) to suggest that it is petrogenetically related to olivine-bearing ultramafic shergottites like ALH 77005. Rocks of the ALH 77005 clan have commonly been called “lherzolitic” shergottites in the literature on Martian meteorites, and in this paper we adhere to this convention, even though these rocks do not contain sufficient orthopyroxene nor the more than 60% olivine necessary to be so named according to established requirements for terrestrial lherzolitic ultramafic rocks (Le Maitre et al., 2002).

In this investigation, preliminary Rb–Sr and Sm–Nd ages reported by Nyquist et al. (2004) for NWA 1460 are refined to 336 ± 15 Ma and 350 ± 16 Ma, respectively. These concordant ages are interpreted as dating the time of crystallization of a thick lava flow on the Martian surface or possibly a feeder dike at shallow depth. The initial Sr and Nd-isotopic compositions of NWA 1460 suggest that its parent magmatic liquid was an earlier melting product of a Martian mantle source region similar to those that produced the “lherzolitic” shergottites and basaltic shergottite EET 79001, lithology B. The Rb/Sr and Sm/Nd ratios in the mantle source regions of the “lherzolitic” shergottites and NWA 1460 were similar, and probably were close to those of bulk Mars.

We also present Ar–Ar data for a plagioclase separate of NWA 1460. Unlike many basaltic shergottites NWA 1460 contains minimal excess, non-radiogenic ^{40}Ar , and this is easily attributable to minor components of either terrestrial or Martian atmospheric composition. Thus, the concordance of the derived Ar–Ar age with the Rb–Sr and Sm–Nd ages at ~ 346 Ma is unambiguous. These data refute the suggestion that generally “young” ages of Martian shergottites should be reinterpreted in light of $^{207}\text{Pb}/^{206}\text{Pb}$ – $^{204}\text{Pb}/^{206}\text{Pb}$ isotopic systematics (Bouvier et al., 2005, 2008). Finally, we examine the implications of the NWA 1460 chronology for impact sampling of the Martian surface, and show that some discrepancy between terrain and meteorite ages remains.

2. PETROLOGY AND SHOCK CHARACTERISTICS

Like NWA 480 (described by Barrat et al., 2002), NWA 1460 is a medium grained mafic igneous rock with an ophitic texture (see Fig. 1). If terrestrial terminology were applied, these rocks would be called diabase or dolerite. Both specimens consist mainly of pyroxene (72 vol.%) and maskelynite (25 vol.%) with accessory merrillite, apatite, titanomagnetite, ilmenite, chromite, pyrrhotite, silica, baddeleyite, and mesostasis K–Al–Si-rich glass. The pyroxene grains in both NWA 480 and NWA 1460 have identical patterns of progressive compositional zonation from magnesian orthopyroxene cores through augite mantles to more ferroan pigeonite rims (Barrat et al., 2002; Irving and Kuehner, 2003), which is the pattern expected for closed system crystallization of mafic igneous magmas of this bulk composition.

Furthermore, the margins of pyroxene grains in NWA 1460 are composed of fine symplectic intergrowths of very Fe-rich clinopyroxene, fayalitic olivine and silica, which are observed also in other basaltic shergottites (Aramovich et al., 2002) and in coarse grained Apollo mare basalts (Ware and Lovering, 1970; Taylor and Misra, 1975). There is a consensus that such intergrowths in essentially unshocked Apollo samples represent subsolidus inversion of former pyroxferroite of igneous origin in relatively slowly-cooled rocks (Lindsley et al. 1972; Aramovich et al., 2002), and therefore no compelling reason exists to suppose that the identical textures in NWA 1460 and other coarse grained basaltic shergottites (including QUE 94201, Los Angeles and NWA 2800) were produced in any other way. Small grains of phosphates, Fe–Ti oxides and baddeleyite with apparently primary igneous crystal morphologies occur within the regions of inverted pyroxferroite in NWA 1460, and thus are interpreted to be late stage igneous minerals that co-crystallized with the rims of the pyroxene grains from evolved residual melt. There is no evidence at scales down to microns for any infiltration by extraneous fluids or alteration of any mineral grains (including phosphates), either on Mars or in the terrestrial desert environment.

Barrat et al. (2002) concluded from pyroxene zoning patterns that NWA 480 and QUE 94201 (an unrelated depleted basaltic shergottite) have very similar igneous cooling histories, and they proposed that the pyroxenes in each rock had grown continuously by single-stage cooling at a slow rate within a closed igneous system. The cosmic-ray exposure (CRE) ages of NWA 480 and NWA 1460 are indistinguishable at 2.6 ± 0.2 Ma (Mathew et al., 2003; Connolly et al., 2006), and also similar to those for QUE 94201, Zagami, Shergotty, and Los Angeles (Eugster et al., 1997, 2002; Nyquist et al., 2001a; Nishiizumi and Caffee, 2006). All Martian meteorites were affected by the shock of impact when they were ejected (converting plagioclase to maskelynite and isolated silica grains to stishovite in shergottites), and some of these rocks also may have experienced shock before their ejection (Treiman et al., 2007; Bogard and Garrison, 2008; Irving et al., 2008; Park et al., 2008). From observation of Ca–Na hollandite grains, which are formed by shock-induced solid-state transforma-



Fig. 1. (a) Upper left: Whole NWA 1460 stone before cutting, showing very fresh fusion crust (photo by Greg Hupé). (b) Upper right: Cut stone (after sampling for isotopic studies), showing fresh interior composed mainly of pale yellowish pyroxene with interstitial gray maskelynite and other phases (photo by Nelson Oakes). (c) Bottom: Plane polarized thin section image (width 15 mm), showing zoned pyroxene (pale brown with darker rims), maskelynite (clear) and opaque phases (mostly titanomagnetite and pyrrhotite) (photo by Ted Bunch).

tion from the original feldspar, Beck et al. (2006) reported that NWA 480 and Zagami experienced intense impact events during ejection with peak shock pressures in the range of 21–23 GPa. Despite the obvious effects of such ejection shock on plagioclase in particular, it can be concluded that the observed compositional zonation within pyroxenes and the integrity and chemistry of the accessory phases within all these specimens were little affected by this short-lived and relatively low temperature shock, and thus truly record Martian igneous processes.

3. SAMPLES AND SAMPLE PREPARATION

The sample processing and preparation protocols are summarized in Fig. 2. The first (“fines”) sample weighing ~130 mg was composed of many small chips with fusion crusts and powdered fines generated during sample processing. These samples were used for a preliminary investigation. After picking out materials with obvious fusion crusts, about 67 mg of the material representing the bulk rock were gently ground. A bulk rock sample, WRf1, was taken. The rest of this sample was treated with warm (~55 °C) 2 N HCl acid for 5 min. Both residues WRf(r) and leachates WRf(l) were analyzed. The rest of the sample chips of ~60 mg with fusion crusts were crushed finely and processed for pyroxene and mask-

elynite separations. A yellowish pyroxene-rich sample (~90% purity) was obtained by density separation using the heavy liquid methylene iodide ($\rho = 3.32 \text{ g/cm}^3$). A lighter clear maskelynite sample (~80% purity) was obtained by flotation with bromoform ($\rho = 2.85 \text{ g/cm}^3$). The pyroxene-rich and maskelynite-rich samples were washed with 2 N HCl and 0.5 N HCl, respectively. Both HCl-washed pyroxene, Pxf(r), and maskelynite, Plagf(r), samples were analyzed.

The second sample of NWA 1460 weighed ~780 mg and was a mostly interior portion of the meteorite. A small corner having exterior material was chipped off. The ~731 mg interior sample was processed for this study following our standard procedures (Nyquist et al., 1994; Shih et al., 1999). The sample was first sonicated in ethanol to remove surface contaminants, and then crushed gently to pass a nylon sieve of opening size <149 μm . About 137 mg was taken as the bulk rock sample (WR2). The rest of the sample was sieved into 149–74 μm and <74 μm size fractions. A maskelynite sample and two pyroxene samples were separated from the finer <74 μm fraction by density separation using heavy liquids of densities $\rho = 2.85 \text{ g/cm}^3$, $\rho = 3.32 \text{ g/cm}^3$, $\rho = 3.55 \text{ g/cm}^3$ (Clerici solution), and $\rho = 4.05 \text{ g/cm}^3$ (Clerici solution). (Clerici solutions were purchased from the Cargille™ Lab, 55 Commerce Road, Cedar Grove, NJ (USA)) The maskelynite sample (Plag) and two pyroxene samples (Px1 and Px2) were concentrated in density fractions of $\rho < 2.85 \text{ g/cm}^3$, $\rho = 3.32\text{--}3.55 \text{ g/cm}^3$, and $\rho = 3.55\text{--}$

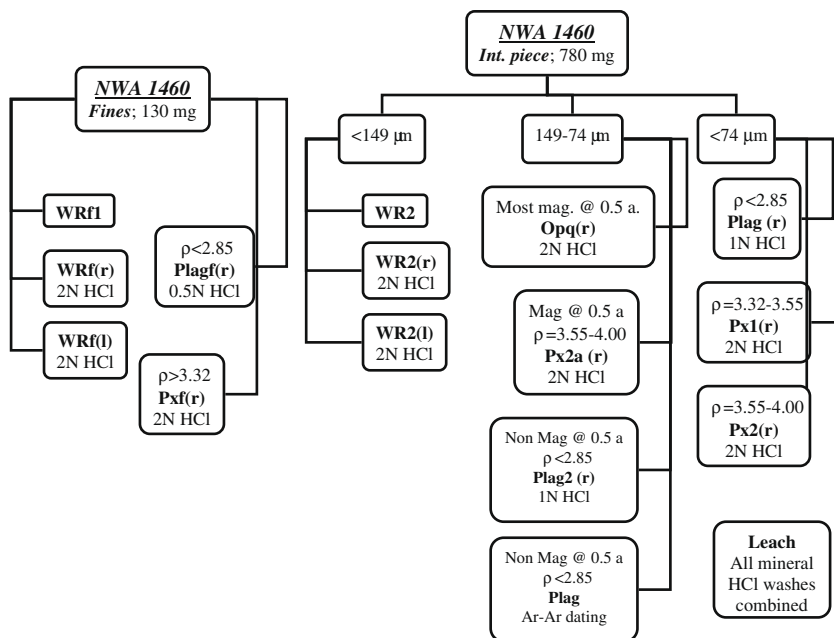


Fig. 2. Sample processing schematic. Mineral separates were from separately processed fines (130 mg) and interior (780 mg) samples. See text for details.

4.05 g/cm³, respectively. Additional mineral samples were separated from the coarser 149–74 μm size fraction by both magnetic susceptibility and density separations. The initial sample of this size fraction was first passed through a Franz separator with the magnet current set at 0.5 Amp. The most magnetic fraction was separated as opaques (Opq). The pyroxene sample (Pxa) was separated by the density fraction $\rho = 3.55\text{--}4.05\text{ g/cm}^3$ of the magnetic portion. The maskelynite sample (Plag2) was separated by the density fraction $\rho < 2.85\text{ g/cm}^3$ of the non-magnetic portion. A 6.2 mg sample of maskelynite was taken for Ar–Ar dating. In order to remove possible terrestrial contaminants due to desert weathering, the bulk rock and all mineral samples were washed with either 1 N HCl (for Plag) or 2 N HCl (for WR2, Pxa and Opq) in an ultrasonic bath for 10 min. Both the WR2 and mineral residues (r) and WR leaches (l) of these samples were analyzed. The acid washes from all minerals (Leach) were combined and also were analyzed.

4. ANALYTICAL PROCEDURES

4.1. Ar–Ar analyses

The 6.2 mg sample of the feldspar (maskelynite) separate was irradiated with fast neutrons in the University of Missouri reactor. The irradiation constant (J -value) was 0.02111 ± 0.00008 , and was determined from multiple irradiated samples of the hornblende age standard, NL-25 (Bogard et al., 1995). Argon was released by stepwise temperature extraction and its isotopic composition measured on a VG-3600 mass spectrometer. Isotopic data were corrected for mass discrimination, system blanks, isotopic decay and reactor interferences, and are given in Table A1 in the Appendix A. Ar–Ar ages were calculated with the decay coefficients given by Steiger and Jäger (1977). Uncertainties indicated for individual ages are propagated from measurement uncertainties in $^{40}\text{Ar}/^{39}\text{Ar}$ ratios and all applied corrections, but do not reflect uncertainties in the J -value, the age of the NL-25 hornblende

($\pm 0.5\%$), or the K decay coefficients. However, the uncertainties in plateau and isochron ages we report are approximately one-sigma and do include the uncertainty in J -value.

4.2. Rb–Sr and Sm–Nd analyses

The detailed sample dissolution techniques and chemical procedures of Rb, Sr, Sm, and Nd separations used in this study were reported previously (Nyquist et al., 1994; Shih et al., 1999). Rb–Sr and Sm–Nd analyses were performed on Finnigan-MAT 261 and 262 mass spectrometers in static-multicollection mode following the procedures of Nyquist et al. (1994). Tantalum oxide slurry was used as an emitter on Re filaments. Nd was analyzed as the oxide (NdO^+). Analyses of the isotopic standards NBS 987 Sr and Ames Nd were interspersed with sample analyses. The typical average values of $^{87}\text{Sr}/^{86}\text{Sr}$ for NBS 987 and $^{143}\text{Nd}/^{144}\text{Nd}$ for Ames Nd metal standard during the course of the study are listed in Table 1. The isotopic data for samples analyzed contemporaneously with the standards were normalized to $^{87}\text{Sr}/^{86}\text{Sr} = 0.710250$ for NBS 987 (Nyquist et al., 1994) and to $^{143}\text{Nd}/^{144}\text{Nd} = 0.511138$ for Ames Nd (Wasserburg et al., 1981). The total procedural blanks for Rb (~ 5 pg), Sr (~ 20 pg), Sm (~ 5 pg), and Nd (~ 10 pg) are low and negligible.

5. ANALYTICAL RESULTS

5.1. Rb–Sr age and initial $^{87}\text{Sr}/^{86}\text{Sr}$

The Rb–Sr analytical results are reported in Table 1. Preliminary data determined on the small, 130 mg sample of “fines” that were mostly created in the process of subdividing the specimen for further analysis were initially reported by Nyquist et al. (2004), and are shown by triangles in Fig. 3. The apparent Rb–Sr age of 312 ± 3 Ma reported by Nyquist et al. (2004) was determined by a single analysis of Pxf(r) shown by an open triangle in Fig. 3. Subsequent analyses

Table 1
The Rb–Sr and Sm–Nd analytical results for shergottite NWA 1460.

Sample ^a	wt. (mg)	Rb (ppm)	Sr (ppm)	⁸⁷ Rb/ ⁸⁶ Sr ^b	⁸⁷ Sr/ ⁸⁶ Sr ^{c,d}	Sm (ppm)	Nd (ppm)	¹⁴⁷ Sm/ ¹⁴⁴ Nd ^b	¹⁴³ Nd/ ¹⁴⁴ Nd ^{f,d}
<i>Fines</i>									
WRf1	31.02	2.54	59.70	0.1230 ± 15	0.709622 ± 18	1.211	2.507	0.29227 ± 29	0.512619 ± 10
WRf(r)	33.35	2.19	40.00	0.1586 ± 21	0.709685 ± 11	0.168	0.216	0.47123 ± 62	0.513024 ± 10
WRf(l) ^g	2.76	4.48	194.00	0.0670 ± 8	0.709531 ± 12	11.3	24.8	0.27563 ± 28	0.512548 ± 10
Pxf(r)	28.86	1.51	7.20	0.6061 ± 31	0.711638 ± 10	0.2066	0.2616	0.47774 ± 89	0.513020 ± 10
Plagf(r)	6.72	7.21	274.00	0.0760 ± 4	0.709309 ± 10	0.3882	0.8688	0.27025 ± 76	0.512489 ± 10
<i>Interior piece</i>									
WR2	26.95	2.36	52.10	0.1308 ± 18	0.709627 ± 10	1.36	2.80	0.29431 ± 30	0.512628 ± 16
WR2(r)	30.95	2.45	44.80	0.1584 ± 23	0.709728 ± 10	0.167	0.216	0.46739 ± 65	0.513004 ± 13
WR2(l) ^g	3.25	1.59	106.00	0.0436 ± 5	0.709413 ± 10	12.5	26.8	0.28138 ± 29	0.512587 ± 17
Plag(r)	19.40	4.15	196.00	0.0614 ± 8	0.709247 ± 10	0.0429	0.113	0.22910 ± 90	0.512368 ± 10
Plag2(r)	9.20	5.72	190.00	0.0873 ± 11	0.709397 ± 10	0.0582	0.125	0.28109 ± 185	0.512554 ± 76
Px1(r)	28.40	1.27	4.60	0.798 ± 16	0.712599 ± 10	0.167	0.197	0.51380 ± 75	0.513109 ± 29
Px2(r)	20.60	1.51	5.44	0.804 ± 15	0.712841 ± 10	0.218	0.242	0.54563 ± 84	0.513160 ± 11
Px2a(r)	37.65	1.16	4.36	0.770 ± 17	0.712535 ± 14	0.218	0.245	0.53958 ± 64	0.513210 ± 10
Opq(r)	8.50	6.76	50.20	0.390 ± 20	0.710893 ± 10	0.104	0.141	0.44396 ± 229	0.512999 ± 81
Leach ^g	6.58	2.96	108.00	0.0792 ± 10	0.709599 ± 10	11.2	24.0	0.28183 ± 29	0.512599 ± 10
NBS 987 Sr	Sr ⁺ (<i>N</i> = 9; 5/03)				0.710224 ± 26 ^e	Ames Nd	NdO ⁺ (<i>N</i> = 9; 6/03)		0.511087 ± 18 ^e
	Sr ⁺ (<i>N</i> = 1; 6/04)				0.710231 ± 22 ^e		NdO ⁺ (<i>N</i> = 12; 5/04)		0.511099 ± 18 ^e
	Sr ⁺ (<i>N</i> = 23; 11–12/05)				0.710275 ± 33 ^e		NdO ⁺ (<i>N</i> = 17; 11–12/05)		0.511154 ± 17 ^e

^a WR, whole rock; Plag, plagioclase; Px, pyroxene; MM, most magnetic; f, fines; l, acid leachate and r, acid-washed residues.

^b Uncertainties correspond to last figures.

^c Normalized to ⁸⁸Sr/⁸⁶Sr = 8.37521 and adjusted to ⁸⁷Sr/⁸⁶Sr = 0.710250 for NBS 987 Sr standard (Nyquist et al., 1990).

^d Uncertainties correspond to last figures and represent ±2σ error limits.

^e Uncertainties correspond to last figures and represent ±2σ error limits. *N*, number of standard runs.

^f Normalized to ¹⁴⁶Nd/¹⁴⁴Nd = 0.724140 and adjusted to ¹⁴³Nd/¹⁴⁴Nd = 0.511138 of the Ames Nd standard (Wasserburg et al., 1981).

^g Leachate weight determined from the difference between the initial sample weight and the residue weight after leaching.

of samples from the interior allocation showed this age to be in error by more than the stated error limits from the isochron regression. We ascribe this discrepancy to the inadvertent inclusion of fusion crust or other material from near the exterior of the sample in the analyses. Nevertheless, these preliminary analyses showed that the Rb–Sr data for NWA 1460 are much less disturbed than usually is the case for hot desert meteorites and even most Antarctic meteorites, consistent with the inference that NWA 1460 must have been a very recent fall.

Data from isotopic analyses of the ~780 mg interior portion of the specimen (see Fig. 2) are shown by circles in Fig. 3. The plagioclase separate was “washed” in 1 N HCl with sonication for 10 min, all other samples were washed in 2 N HCl. One bulk sample (WR2) was analyzed without washing. A second bulk sample was washed to yield leachate WR2(l) and residue WR2(r). The acid washes of mineral separates were combined for the “Leach” sample. The elevated ⁸⁷Sr/⁸⁶Sr ratios of the leachates show the probable presence of terrestrial Sr contamination. Leachate data are shown as open symbols in Fig. 3, and are omitted from the isochron regression. An age of 336 ± 15 Ma is determined by regressing the analyses of the residues after leaching for whole rock, plagioclase, pyroxene, and magnetic “opaques” (solid symbols in Fig. 3). Initial ⁸⁷Sr/⁸⁶Sr = 0.708968 ± 30 obtained for these combined data for the two samples agrees with 0.708979 ± 10 and 0.708980 ± 30, respectively, obtained when the data for the “fines” and interior samples are sep-

arately regressed. Thus, Sr was isotopically equilibrated throughout the rock during its crystallization from magma. Plagioclase, with a modal abundance of ~25% and Sr concentration of ~193 ppm is the major host of Sr in the rock. For example, plagioclase alone could account for ~93% of the measured Sr abundance of 52 ppm in WR2. The Sr concentration in the leachate WR2(l) was more than twice that in the residue WR2(r), the majority of which could have been terrestrial contamination. WR2(l) also would have contained Sr from phosphates, possibly accounting for part of the elevated Sr concentration. However, these data were excluded from the isochron calculation because of the high probability the leachates contained some contaminant Sr. The isochron regression of the preferred data set (solid symbols in Fig. 3) thus is interpreted as giving the crystallization age of NWA 1460 as 336 ± 15 Ma for initial ⁸⁷Sr/⁸⁶Sr = 0.708968 ± 30.

The initial ⁸⁷Sr/⁸⁶Sr of NWA 1460 is similar to those of “Iherzolitic” shergottites ALH 77005 and LEW 88516 (0.710260 ± 40 and 0.710520 ± 40, respectively; Borg et al., 2002) as well as basaltic shergottite EET 79001(B) (0.712564 ± 11; Nyquist et al., 2001b). As discussed more extensively below, a two-stage model gives time-averaged ⁸⁷Rb/⁸⁶Sr ~0.16 for the mantle source of NWA 1460, ~10% lower than for the “Iherzolitic” shergottites, ~22% lower than for EET 79001, and identical to that estimated for bulk Mars by Borg et al. (1997). An independent estimate of ⁸⁷Rb/⁸⁶Sr ~0.13 for bulk Mars was made by Shih et al. (1999).

5.2. Sm–Nd age and initial $^{143}\text{Nd}/^{144}\text{Nd}$

Fig. 4 reports the Sm–Nd data obtained for both the ~130 mg subsample of “fines” (triangles) and the ~780 mg interior subsample. For the “fines” sample, the plagioclase residue analysis (Plagf(r)) lies slightly off the isochron determined by the majority of the combined data for the two samples (solid symbols). For the “fines” sample, we prefer the data for the whole rock (WRf) and whole rock leachate (WRf(l)) samples because they contained more Nd for analysis, and thus were less susceptible to contamination, blank, or unknown processing difficulties. Moreover, the Nd and Sm abundances for Plagf(r) are much higher than those found subsequently for plagioclase separated from the ~780 mg sample, leading to the suspicion of the presence of an uncharacterized phase, possibly a contaminant.

The Sm–Nd isotopic data for the ~780 mg sample are shown by circles in Fig. 4. As for the earlier sample, one of the plagioclase analyses (Plag(r)) falls off the isochron. This separate was a “float” from the <74 μm size fraction of the ~780 mg subsample (cf. Fig. 2). Because the direction of deviation from the whole rock (WR) and leachate data is the same as for the Plagf(r) analysis of the “fines” sample, we tentatively ascribe this behavior to a real phase or effect that is apparent only for plagioclase samples, which have very low rare earth element (REE) abundances. We note that the Plag(r) sample has the lowest measured Sm and Nd abundances among all the samples (~0.1 ppm), and thus was most susceptible to addition of extraneous phases. Plag(r) is furthest displaced in the direction of a hypothetical extraneous phase. A possible candidate for such a phase is molten plagioclase glass from near the fusion crust of the sample. Although the Plag(r) data fall off the isochron, data for a second plagioclase sample of the ~780 mg specimen (Plag2(r)) fall on the isochron, reinforcing the interpretation of random contributions of an uncharacterized phase to Plag(r) and Plagf(r). The Nd and Sm concentrations in Plag(r) are the lowest among

the plagioclase samples. This observation suggests that the “uncharacterized phase” is a component of isotopically disturbed plagioclase, consistent with it being molten plagioclase from a volume of the meteorite near the fusion crust. An isochron fit to the data shown as solid symbols yields an age $T = 350 \pm 16$ Ma and $\epsilon_{\text{Nd}} = 10.6 \pm 0.5$.

We note that the Nd concentration in leachate WR2(l), for example, is ~240 times higher than in the plagioclase samples, so the phosphates contributing to WR2(l) were much less susceptible to terrestrial contamination or other disturbances than the plagioclase samples. Further, the coincidence of Sm–Nd isotopic data for plagioclase (Plag2(r)) and phosphates (leachates) shows that the phosphates present in NWA 1460 were produced by igneous crystallization (cf. Wadhwa et al., 1994). Although Pxf(r) from the ~130 mg sample likely was relatively impure, the data for the other pyroxene residue samples were very reproducible. The Sm–Nd data for the small sample of “opaques” separated as the most magnetic fraction of the ~780 mg whole rock sample also lies on the isochron near the whole rock residue. The relatively high REE content of this separate likely results from baddeleyite inclusions, which are observed to be commonly associated with ilmenite in this specimen (Irving and Kuehner, 2003). The excellent reproducibility of the Sm–Nd data for the two subsamples supports the interpretation of the Sm–Nd age as a measure of the crystallization age of NWA 1460. The Sm–Nd age of 350 ± 16 Ma agrees with the Rb–Sr age of 336 ± 15 Ma within their respective error limits, and we interpret both as independent measures of the crystallization age of NWA 1460.

5.3. Ar–Ar plateau age

The sample used for Ar–Ar analysis was a plagioclase (maskelynite) separate equivalent to Plag2 used for the Rb–Sr and Sm–Nd analyses, except that it was not washed

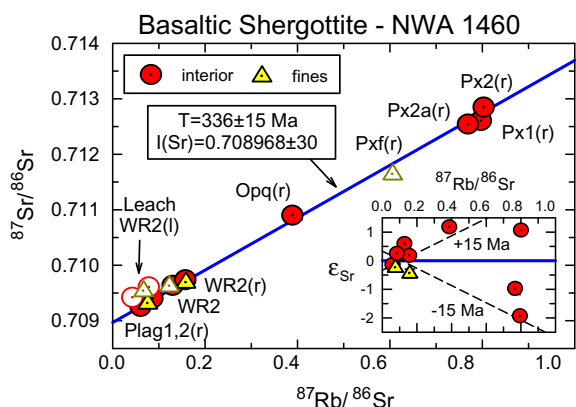


Fig. 3. Rb–Sr isochron for NWA 1460. Triangles denote data from a first allocation of sample “fines”. Circles denote data from a second, larger allocation of the bulk specimen. Solid symbols denote data included in the isochron regression, open symbols data excluded from the regression.

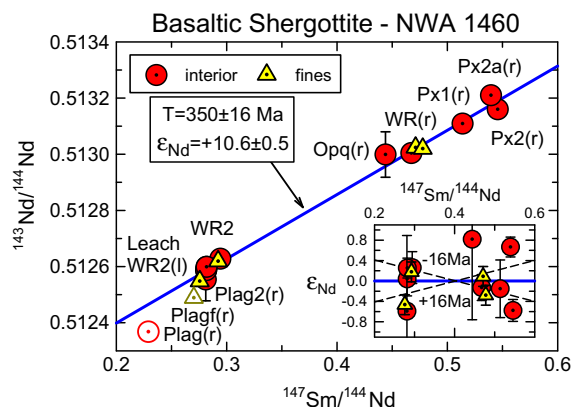


Fig. 4. Sm–Nd isochron for NWA 1460. Circles denote data from the second, larger allocation of the bulk specimen. These data are labeled in the figure. Triangles denote data from a first allocation of sample “fines”. From left to right in the figure, these data are for Plagf(r), WRf(l), WRf1, WRf(r), and Pxf(r), resp. (See Table 1.) Solid symbols denote data included in the isochron regression, open symbols data excluded from the regression.

in 1 N HCl (see Fig. 2). The ^{39}Ar – ^{40}Ar age spectrum for NWA 1460 plagioclase is given in Fig 5. The first few temperature extractions showed higher values of the K/Ca and $^{36}\text{Ar}/^{37}\text{Ar}$ ratios, which suggest effects of terrestrial weathering of grain surfaces often observed in hot desert meteorites. However, 14 extractions releasing 9–100% of the ^{39}Ar give a constant K/Ca ratio of 0.0422 ± 0.0039 suggesting gas release from a single (plagioclase) phase unaffected by weathering. Release of terrestrial ^{40}Ar probably accounts in part for the much higher Ar–Ar ages for those extractions releasing 0–9% of the ^{39}Ar . Seven extractions releasing 41–98% of the ^{39}Ar define an average plateau age of 360 ± 6 Ma (1σ), which is an upper limit to the Ar–Ar age of NWA 1460. The last extraction (1400 °C, releasing <1% of the ^{39}Ar) gives a much higher and more uncertain age due to the smaller extracted gas amount and a higher blank. This Ar–Ar plateau age is within uncertainties equal to the Sm–Nd age of 350 ± 16 Ma, but slightly exceeds the Rb–Sr age of 336 ± 15 Ma. This observation suggests that the Ar–Ar data should be examined more closely for evidence of trapped Martian mantle-derived ^{40}Ar as has been observed for other shergottites (Bogard and Park, 2008a).

5.4. Ar–Ar isochron age

To characterize the likely presence of excess ^{40}Ar in NWA 1460 Plag, we utilize isochron plots. For terrestrial samples, a plot of $^{40}\text{Ar}/^{36}\text{Ar}$ vs. $^{39}\text{Ar}/^{36}\text{Ar}$ often is used to resolve ^{40}Ar arising from *in situ* decay of ^{40}K from excess ^{40}Ar incorporated from some other source. For most such isochrons, the slope is proportional to the age and the $^{40}\text{Ar}/^{36}\text{Ar}$ intercept measures a trapped component not produced *in situ*. However, isochrons for Martian meteorites are more complex. Martian meteorites usually contain two or more of the following ^{36}Ar components: cosmogenic ^{36}Ar , ^{36}Ar from the terrestrial atmosphere released at low temperatures, ^{36}Ar from the Martian atmosphere, and

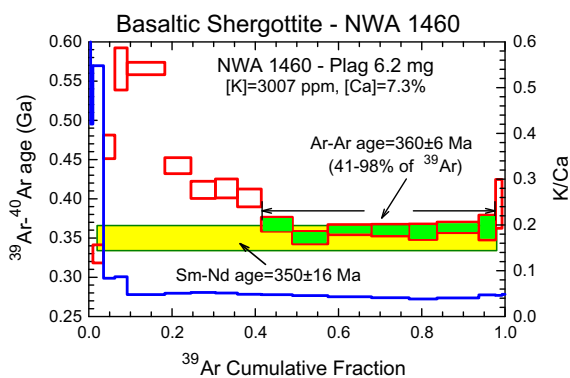


Fig. 5. Ar–Ar age plateau. ^{39}Ar – ^{40}Ar ages (rectangles, left axis) and K/Ca ratios (stepped (blue) line, right axis) for stepwise temperature extractions of a plagioclase separate of NWA 1460. Seven extractions releasing 41–98% of the ^{39}Ar define an age of 360 ± 6 Ma. The corresponding plateau ages are shown by (green) shaded boxes. The ages shown by open boxes were excluded from the average. (For interpretation of the references to color in this figure legend, the reader is referred to the web version of this article.)

^{36}Ar from the Martian interior. The presence of more than one ^{36}Ar component can produce scatter in the isochron. Often the minimum measured $^{36}\text{Ar}/^{37}\text{Ar}$ ratio for feldspar may represent a pure nuclear component, where all ^{36}Ar arises from cosmogenic production from Ca in space, and ^{37}Ar is produced from Ca in the reactor. Using this defined nuclear $^{36}\text{Ar}/^{37}\text{Ar}$ ratio, the ^{36}Ar in those extractions showing higher ratios then can be divided into cosmogenic and trapped components (Garrison et al., 2000). Alternatively, if the concentration of cosmogenic ^{36}Ar has been measured in an un-irradiated sample, then this value may be used to define the nuclear $^{36}\text{Ar}/^{37}\text{Ar}$ ratio and to separate ^{36}Ar into components. Note that even in this case, the “trapped component” can be itself a multi-component mixture.

Isochron normalization to trapped ^{36}Ar ($^{36}\text{Ar}_{\text{tr}}$) can be made for samples which contain significant $^{36}\text{Ar}_{\text{tr}}$. Normalization to ^{37}Ar is preferred for samples which contain little $^{36}\text{Ar}_{\text{tr}}$ but whose K/Ca ratios vary significantly throughout the extractions (Bogard and Park, 2008a). For NWA 1460 plagioclase, cosmogenic ^{36}Ar ($^{36}\text{Ar}_{\text{cos}}$) is a significant component, and the K/Ca ratio is essentially constant for most of the Ar release. As a result, isochrons normalized to $^{36}\text{Ar}_{\text{cos}}$ or ^{37}Ar produce little dispersion in the ratios, and the slopes are not well defined. We thus are forced to normalize to $^{36}\text{Ar}_{\text{tr}}$ by identifying $^{36}\text{Ar}_{\text{cos}}$ and subtracting it from total ^{36}Ar . We identify $^{36}\text{Ar}_{\text{cos}}$ in two ways. In the first method (#1) we assume that the minimum measured $^{36}\text{Ar}/^{37}\text{Ar}$ ratio (0.000589 at 990 °C), which occurs at the peak of the ^{37}Ar release, represents a pure nuclear component (i.e., all ^{36}Ar is cosmogenic). We then use measured $^{36}\text{Ar}/^{37}\text{Ar}$ ratios to correct all other extractions for this $^{36}\text{Ar}_{\text{cos}}$ component (see Garrison et al., 2000). We must omit the 990 °C datum from the isochron, as it has been defined as having no $^{36}\text{Ar}_{\text{tr}}$.

As a second method (#2) of determining $^{36}\text{Ar}_{\text{tr}}$, we estimate a total $^{36}\text{Ar}_{\text{cos}}$ concentration for NWA 1460, for which cosmogenic noble gases have not been reported. The CRE age for the paired meteorite NWA 480, from analyses of both cosmogenic noble gases (Mathew et al., 2003) and ^{10}Be (Nishiizumi and Caffee, 2006), is similar to, if not identical to, CRE ages for “enriched” basaltic shergottites Zagami, Shergotty, and Los Angeles (Eugster et al., 1997, 2002). Several analyses of Shergotty and Zagami in various laboratories gave a range in $^{36}\text{Ar}_{\text{cos}}$ concentrations of 1.77 – $2.49 \times 10^{-9} \text{ cm}^3/\text{g}$ for whole rock samples and 1.50 – $2.71 \times 10^{-9} \text{ cm}^3/\text{g}$ for feldspar separates (Eugster et al., 1997; Terribilini et al., 1998; Park and Nagao, 2003; Park, 2005; Schwenzer et al., 2007). Variations in these $^{36}\text{Ar}_{\text{cos}}$ values are to be expected because of variable sample composition and space shielding among individual samples. The overall average of 10 measurements is $2.15 \times 10^{-9} \text{ cm}^3/\text{g}$, which is the $^{36}\text{Ar}_{\text{cos}}$ value we adopt for our NWA 1460 sample. This $^{36}\text{Ar}_{\text{cos}}$ value defines a pure nuclear $^{36}\text{Ar}/^{37}\text{Ar}$ ratio of 0.000456, which would suggest all extractions of NWA 1460 released small amounts of $^{36}\text{Ar}_{\text{tr}}$.

Fig. 6 shows the isochron plots for extractions releasing 6–98% of the ^{39}Ar and normalized to $^{36}\text{Ar}_{\text{tr}}$, obtained by both of these methods (#1 and #2) of determining $^{36}\text{Ar}_{\text{tr}}$ concentrations. Most of the uncertainties indicated in the ratios arise from the ^{36}Ar values, not the $^{39}\text{Ar}/^{40}\text{Ar}$ ratios

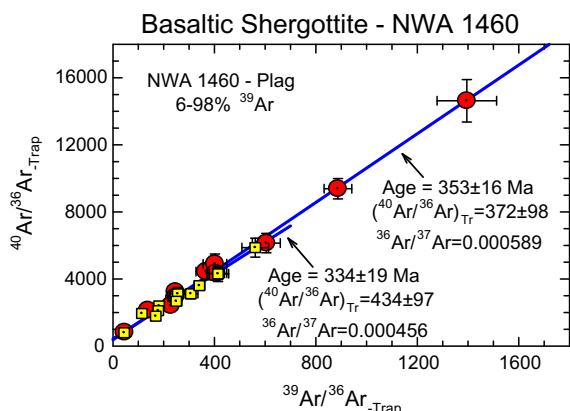


Fig. 6. Ar–Ar isochron-age for 12 extractions releasing 6–98% of the ^{39}Ar . The concentrations of trapped ^{36}Ar were obtained by subtracting the cosmogenic ^{36}Ar component from total ^{36}Ar as estimated in two alternative ways. (a) The minimum $^{36}\text{Ar}/^{37}\text{Ar}$ ratio as measured for the 990 °C extraction (Table A1) was used to estimate a “nuclear” $^{36}\text{Ar}/^{37}\text{Ar} = 0.0005891$ for the reactor-irradiated plagioclase. The slope of the corresponding isochron defines an age of 353 ± 16 Ma. (Solid (red) circles.) (b) Independently determined estimates of cosmogenic ^{36}Ar were used to estimate nuclear $^{36}\text{Ar}/^{37}\text{Ar} = 0.000456$. The slope of an isochron obtained in this manner defines an age of 334 ± 19 Ma. (Small (yellow) squares. See text.) (For interpretation of the references to color in this figure legend, the reader is referred to the web version of this article.)

on which the age depends. Nevertheless, we calculated the isochron slope by weighting each plotted point by its uncertainties, according to the method of Williamson (1968). The Ar–Ar age determined by using the minimum measured $^{36}\text{Ar}/^{37}\text{Ar}$ ratio to calculate $^{36}\text{Ar}_{\text{tr}}$ (method #1) is 353 ± 16 Ma. The isochron age obtained by not weighting individual points with their uncertainties is 346 ± 6 Ma. If we use an estimated $^{36}\text{Ar}_{\text{cos}}$ concentration to calculate $^{36}\text{Ar}_{\text{tr}}$ (method #2), the Ar–Ar age is 334 ± 19 Ma. We also examined an “isochron” produced by plotting the ^{40}Ar concentration versus the ^{39}Ar concentration for extractions releasing 0–98% of the ^{39}Ar , which removes uncertainties associated with normalization to $^{36}\text{Ar}_{\text{tr}}$. The slope of this plot gives an unweighted age of 358 ± 3 Ma and an excess

^{40}Ar intercept of $\sim 3 \times 10^{-8} \text{ cm}^3/\text{g}$. Within combined uncertainties, these isochron ages all overlap with each other and with the plateau age (Table 2).

Because essentially all of the $^{40}\text{Ar}_{\text{tr}}$ degassed below $\sim 41\%$ ^{39}Ar release, we examined separately isochrons for 6–41% and 41–98% of the ^{39}Ar , where trapped ^{36}Ar was obtained by both methods #1 and #2. These results also are shown in Table 2. Both determinations for 41–98% ^{39}Ar release give ages only very slightly less than the plateau age and low (but uncertain) trapped $^{40}\text{Ar}_{\text{tr}}$, and that the true Ar–Ar age may be only slightly less than the plateau age. Isochron ages for 6–41% ^{39}Ar release obtained by both methods are higher than the plateau age. These cannot be real ages, because they exceed the plateau age and because they are most affected by $^{40}\text{Ar}_{\text{tr}}$. The $^{40}\text{Ar}/^{36}\text{Ar}$ intercepts for those isochrons including the greatest amount of $^{40}\text{Ar}_{\text{tr}}$ (6–41% ^{39}Ar), suggest values similar to the terrestrial atmospheric value or larger, although the uncertainties are large. The concentration of ^{40}Ar from *in situ* decay is considerably greater than the total concentration of trapped ^{40}Ar , which is unlike the situation for all shergottites containing Martian atmospheric ^{40}Ar and many shergottites containing trapped interior Ar. Trapped Ar released over the first several extractions may have been a mixture of terrestrial and Martian atmospheric components.

These various ways of examining the Ar–Ar data utilized nearly all extractions and indicate that the true NWA 1460 age lies between the upper age limit defined by the 360 Ma plateau age and the age of 334 ± 19 Ma obtained using method #2 to obtain $^{36}\text{Ar}_{\text{tr}}$. If we average the four isochron ages of <360 Ma and consider the plateau age to be an upper limit, we obtain a preferred Ar–Ar age of 351 ± 15 Ma. The 1σ uncertainty in this age reflects the maximum error on the plateau age and almost overlaps with the lowest age obtained. Because the lowest isochron age of 334 Ma includes $^{40}\text{Ar}_{\text{tr}}$ released at lower temperatures and assumes a greater concentration of trapped ^{36}Ar , it may have been affected by uncorrelated release of both terrestrial and Martian $^{40}\text{Ar}_{\text{tr}}$ with different $^{40}\text{Ar}/^{36}\text{Ar}$ ratios. Thus, all three independent methods (Rb–Sr, Sm–Nd, and Ar–Ar) give concordant ages for NWA 1460. A

Table 2
NWA 1460 $^{39}\text{Ar}/^{40}\text{Ar}$ age summary.

Type, ^{39}Ar range	$(^{36}\text{Ar})_{\text{cos}}/^{37}\text{Ar}$	Age (Ma)	\pm	$^{40}\text{Ar}/^{36}\text{Ar}$	\pm
Plateau, 41–98%	NA	360	6	NA	NA
Isochron, 6–98%	0.000589	353	16	372	98
Isochron, 6–98%	0.000456	334	19	434	97
Isochron, 41–98%	0.000589	359	27	34	400
Isochron, 41–98%	0.000456	358	42	35	389
Isochron, 6–41%	0.000589	390	34	311	121
Isochron, 6–41%	0.000456	375	38	321	124
K–Ar Iso, 0–98%	NA	358 ^a	3 ^a	NA	
Preferred values	NA	351	15	<530	

Uncertainties are approx. 1σ and include the uncertainty in J -value. NA, not applicable.

^a The K–Ar isochron is unweighted.

similar Ar–Ar age obtained for the early Ar extractions demonstrates that significant radiogenic $^{40}\text{Ar}^*$ loss from the mafic magma did not occur.

6. DISCUSSION

6.1. Concordant radiometric ages for NWA 1460 determine its crystallization age

The good agreement among the radiometric ages of NWA 1460 reported here by different techniques implies that they are valid measures of its formation age. The different techniques depend on different mineral phases to varying degrees, yet all give the same age. Bouvier et al. (2005, 2008) reported Pb-isotopic data for shergottites which apparently give a much older age. They argue that the Pb isotopic compositions of the leached whole-rock fragments and maskelynite separates of Zagami, Shergotty, Los Angeles and other shergottites fall on a whole-rock $^{207}\text{Pb}/^{206}\text{Pb}$ isochron and collectively yield a Pb–Pb age of 4050 ± 70 Ma for the crystallization of the basaltic shergottite suite. They argue further that the contrast between younger ages given by internal isochrons for the shergottites and the ~ 4.1 Ga age indicated by the $^{207}\text{Pb}/^{206}\text{Pb}$ isochron and a whole rock Rb–Sr “isochron” for shergottites simply reflects isotopic perturbation. They maintain that internal Rb–Sr, Sm–Nd, Lu–Hf, and U–Pb “errorochrons” are heavily biased by the presence of disseminated phosphate minerals and inclusions. The isotopic systematics of these minor phases are hypothesized to have been reset either by percolating Martian ground waters (Bouvier et al., 2005), or by impact metamorphism (Bouvier et al., 2008).

The Pb-isotopic data that form the basis for the discussions by Bouvier et al. (2005, 2008) predominantly come from the “enriched” basaltic shergottites Zagami, Shergotty, and Los Angeles, which share common crystallization and ejection ages of ~ 170 Ma and ~ 2.8 Ma, respectively (cf. Nyquist et al., 2001a). Thus, these meteorites likely were ejected in a common event, and could in principle have shared a unique history of isotopic resetting on Mars. However, Bouvier et al. (2005) extended their scenario to include EET 79001, a basaltic shergottite of similar crystallization age to the others, but with an ejection age of only ~ 0.7 Ma, and thus presumably from a different geological site on Mars. Bouvier et al. (2008) further extended the hypothesis to include essentially all known shergottites on their whole rock Rb–Sr “isochron”, including NWA 1460. By supposition, Bouvier et al. (2008) claim that all of the diverse shergottite lithologies were formed at ~ 4.1 Ga ago and were isotopically reset to varying degrees to obtain varying radiometric ages. However, because shergottites were ejected from Mars at different times, with up to 4 events occurring in the period from ~ 0.7 to ~ 4.5 Ma ago (cf. Christen et al., 2005; Park, 2005) isotopic resetting would have to be a very common occurrence connected either with ongoing Martian processes, or with the ejection events themselves.

Bouvier et al. (2005) hypothesized that isotopic resetting affecting phosphate minerals might be connected with the

last dry-out of Martian lakes. In response to reports of “young” Pb–Pb ages for shergottite baddeleyites determined by *in situ* analyses (Herd et al., 2007; Misawa and Yamaguchi, 2007), Bouvier et al. (2008) also advanced the alternative hypothesis that the young ages reflected impact resetting by shock either during ejection of the shergottites from Mars, or possibly during a cluster of impact events on the Martian surface due to the breakup of a “nearby” asteroid in the inner regions of the main asteroid belt (cf. Bottke et al., 2007). Because the isotopic systematics of NWA 1460 are particularly unambiguous they are well suited to an examination of these hypotheses. In the following sections we consider why each of the ages determined here separately yields a valid determination of the formation age of NWA 1460. This result contradicts hypotheses that its ~ 346 Ma age is a consequence of isotopic resetting, and calls into question attempts to explain the young ages of other shergottites in that manner.

6.1.1. Validity of the Rb–Sr age

Bouvier et al. (2005) attributed hypothetically reset Rb–Sr ages of shergottites to exchange of Sr between ground-water and phosphates in the rocks. This suggestion is untenable on several counts. First, phosphates are not a major contributor to the Rb–Sr budget in shergottites, as shown by the data in Table 1. The 2 N HCl leaching procedure used for the NWA 1460 analyses has been found to be effective for dissolving most phosphates for Sm–Nd analyses. For hot desert meteorites like NWA 1460, this leach step inevitably contains some terrestrial Sr contamination, but in the case of NWA 1460, such contamination was minor. The Rb–Sr data for the leachates plot close to the isochron determined for the other mineral phases (Fig. 3, WRf(1), WR2(1), and “leach”). The Sr concentrations in these leachates were lower by about one and one-half to twofold than in the plagioclases, and since the modal abundance of (apatite + merrillite) in the rock (~ 0.5 vol.%) is much less than that of plagioclase, the contribution of phosphates to the Sr budget of the rock is minor. In any case, leachate (“phosphate”) data were not included in the isochron regression. The isochron age is determined only by the pyroxene and maskelynite analyses.

The pyroxene mineral separates of NWA 1460 have the highest $^{87}\text{Rb}/^{86}\text{Sr}$ and $^{87}\text{Sr}/^{86}\text{Sr}$ ratios and plagioclase the lowest ratios among the samples analyzed (Fig. 3). The data for these two minerals together control the slope of the isochron, and therefore the calculated age. No accessible phosphates were included in the pyroxene analyses, since the pyroxene separates were all washed in HCl prior to analysis. In a study of the Rb–Sr isotopic systematics of phosphates in ordinary chondrites, Podosek and Brannon (1991) demonstrated that phosphates would be quantitatively removed by etching phosphate-enriched samples with 0.5 N HCl for about 20 min at room temperature. In the current study, all bulk rock and pyroxene samples were etched in a stronger 2 N HCl with sonication for 10 min. Using this more severe etching procedure, all accessible phosphate contaminants in the bulk rock and pyroxene samples should have been removed. Also, the $^{87}\text{Rb}/^{86}\text{Sr}$ ratios in NWA 1460 leachates (phosphates) are low, so any

inaccessible, unleached phosphates could not have controlled the Rb–Sr data of the pyroxene separates. $^{87}\text{Rb}/^{86}\text{Sr}$ ratios in the NWA leachates are similar to those reported for phosphates in chondrites (Podosek and Brannon, 1991; Rotenberg and Amelin, 2001, 2002). Both subsamples of NWA 1460 leachates of the bulk rock have $^{87}\text{Rb}/^{86}\text{Sr}$ ratios in the range of $\sim 0.04\text{--}0.07$ (Table 1). The mineral washes of the ~ 780 mg sample, including the pyroxene separates, were combined and analyzed as “Leach” (Table 1 and Fig. 3). $^{87}\text{Rb}/^{86}\text{Sr} \sim 0.08$ for this sample was similar to that for the other leachates (WRf(l) and WR2(l)) confirming that phosphates were likely the major Rb–Sr carrier in the pyroxene leachates. Moreover, phosphates inadvertently included with the pyroxene residues (Px(r)) could not be the cause of the high measured $^{87}\text{Rb}/^{86}\text{Sr}$ ratios of the latter, and thus could not have controlled the position of the “high points” on the Rb–Sr isochron.

Phosphates also could not have controlled the position of the “low points” on the isochron, i.e., the plagioclase data. During crystallization of the rock, Sr was mostly partitioned into the plagioclase. Fig. 7 shows that Sr partitioning was very reproducible for shergottites. It plots the molar Sr/Ca ratio in shergottite maskelynite as a function of the Sr concentration in the maskelynite. Fig. 7 shows that the molar Sr/Ca ratio is approximately constant at about 1 per mil for maskelynite separates from basaltic shergottites. The Sr concentration in NWA 1460 maskelynite (190–196 ppm for the 780 mg subsample) is very similar to that for Zagami maskelynite, for example. Such constancy would not be expected if the Sr had been picked up from circulating Martian brines, for the action of which there is no petrological evidence. Fig. 7 shows that Sr obeys the rules expected for partitioning between maskelynite and melt during igneous processes. For example, Blundy and

Wood (1991) showed that at An ~ 0.5 , the plagioclase/melt partition coefficient D_{Sr} is >1 for plagioclase in a range of rock types. Because D_{Sr} is >1 , the Sr concentration in the melt will be lowered as plagioclase crystallizes. Thus, the Sr abundance in maskelynite will be less for a given Sr/Ca ratio for more evolved magmas like those parental to Dhofar 378 and Los Angeles for which plagioclases have lower An and higher Ab contents than plagioclases from the Zagami parent melt, for example. Also, because the albite partition coefficient $D_{\text{Ab}} > D_{\text{An}}$, plagioclase of lower An content will have higher Sr/Ca ratios for a given Sr concentration, as observed in Fig. 7. The atypically high Sr (and Rb) concentration of the ~ 6.7 mg Plagf(r) separate probably reflects unrepresentative sampling of zoned plagioclase. These observations reinforce the essential point that the Sr abundances in shergottite maskelynites were established by mineral/melt partitioning as the parental magma crystallized. Thus, we conclude that the Sr (and Rb) abundances in the mineral phases of NWA 1460 result from elemental partitioning during its igneous crystallization, and that the Rb–Sr isochron reflects the igneous crystallization age of NWA 1460, not the time of any putative groundwater interaction with phosphates.

6.1.2. Validity of the Sm–Nd age

The Sm–Nd isochron age is potentially most susceptible to resetting by groundwater interaction because phosphates are relatively easily weathered and have high REE abundances. The Nd abundance in the bulk rock leachate WR2(l) is $\sim 10\times$ greater than in bulk rock sample WR2 (Table 1). Fig. 8 shows the concentrations of Rb, Sr, Sm, and Nd in mineral separates of NWA 1460 normalized to those in whole rock sample WR2, and compared to similar representations for lunar basaltic meteorites, MIL 05035 and LAP 02205. We note first that trace elements are more strongly partitioned among mineral phases in this Martian rock than in the lunar basalts used for comparison.

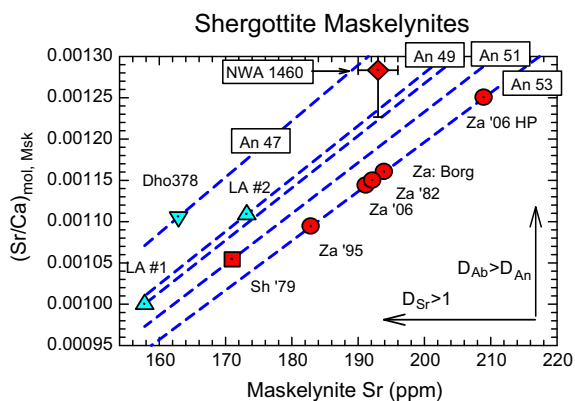


Fig. 7. Molar Sr/Ca ratios in maskelynite separates from basaltic shergottites. Plagioclase compositions are from the following references: Shergotty: Stolper and McSween (1979) and Nyquist et al. (1979); Zagami: Stolper and McSween (1979); Los Angeles: Warren et al. (2004); Dho 378: Ikeda et al. (2006); NWA 1460: This investigation. Dashed (blue) lines show the effect of varying Sr concentrations within plagioclase of constant An content. Sr was partitioned into shergottite plagioclase as expected for mineral/melt partitioning during igneous crystallization. (For interpretation of the references to color in this figure legend, the reader is referred to the web version of this article.)

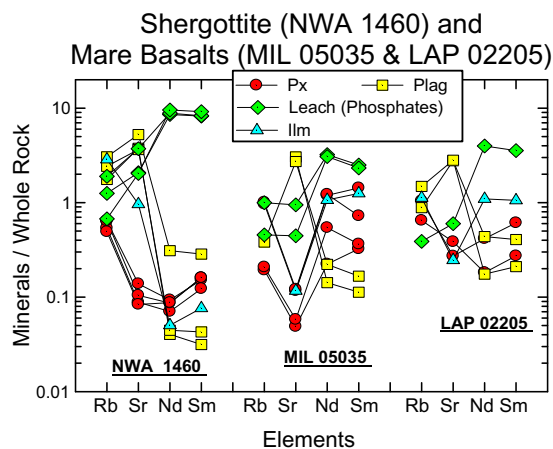


Fig. 8. Concentrations of Rb, Sr, Sm, and Nd in mineral separates of NWA 1460 normalized to those in whole rock sample W2, and compared to similar representations for two lunar meteorites MIL 05035 and LAP 02205. Element partitioning in the Martian basalt resembled that in the lunar basalts, being governed by igneous partitioning. All data are from the JSC laboratory.

Although we have not attempted to model the partitioning in detail, it is clearly a function of the detailed mineralogy and crystallization sequence for the rocks. Second, any weathering by Martian groundwater would be expected to lower REE abundances in the most easily susceptible phosphates, and increase them in relatively susceptible feldspar, whereas this would not be a factor for the lunar basalts. Fig. 8 shows no evidence that the trace element abundances in NWA 1460 might have been affected in such a way, whereas the abundances in the lunar basalts were not. In fact, Nd and Sm are more strongly differentially partitioned between plagioclase and the leachates than is the case for the lunar basalts. Third, there is no evidence that the REE abundances in pyroxene separates were affected by external factors either. The Sm–Nd isochron of Fig. 4 is determined by high Sm/Nd pyroxenes and low Sm/Nd plagioclase and (phosphate) leachates. The Sm and Nd concentrations in plagioclase and phosphates differ by more than two orders of magnitude, yet their isotopic systematics are nearly identical, and anchor the lower end of the Sm–Nd isochron. Thus, the Sm–Nd isochron, like the Rb–Sr isochron, must result from trace element partitioning during igneous crystallization, and thus dates crystallization of NWA 1460.

Independently of these geochemical arguments, the Sm–Nd isotopic data alone preclude an old age near 4.1 Ga for NWA 1460. Fig. 9 illustrates the effect of “correcting” the Sm–Nd isotopic data of NWA 1460 pyroxene separate Px2(r) for a hypothetical admixture of “young” phosphate-borne contaminant Sm and Nd. Lacking reliable data from other mineral phases, a CHUR model age giving the approximate time of fractionation of the Sm/Nd ratio in pyroxene from the chondritic value present in an initially undifferentiated Mars could be calculated. The upper bound on pyroxene model ages is ~ 575 Ma as calculated for the “uncorrected” Px2a(r) analysis (Table 1). “Correcting” for increasingly greater degrees of contamination by phosphate-borne Sm and Nd with a low $^{147}\text{Sm}/^{144}\text{Nd}$ ratio has the effect of moving the pyroxene datum to the right in the diagram, thereby generating increasingly younger model ages, each of which becomes an hypothetical upper bound on the crystallization age. Thus, the Sm–Nd data of NWA 1460 pyroxenes, expected to be robust against either groundwater metasomatism or shock-related thermal metamorphism, cannot be made compatible with an age close to 4.1 Ga.

6.1.3. Validity of the Ar–Ar age

Bouvier et al. (2008) suggested that older apparent Ar–Ar ages in most shergottites, compared to ages determined by other techniques, are the consequence of incomplete degassing of ^{40}Ar from ~ 4.1 Ga-old rocks. To support their contention, they considered the Ar isotopic data reported by Walton et al. (2007, Appendix A) from their laser probe ^{39}Ar – ^{40}Ar study of the shergottites Zagami, Los Angeles, Dar Al Gani 476, and Northwest Africa 1068. Apparent ^{39}Ar – ^{40}Ar ages (uncorrected for atmospheric Ar) measured by Walton et al. (2007) for melt pockets in these meteorites tend to be older than the apparent ages of surrounding minerals. Bouvier et al. (2008) argue that these old apparent

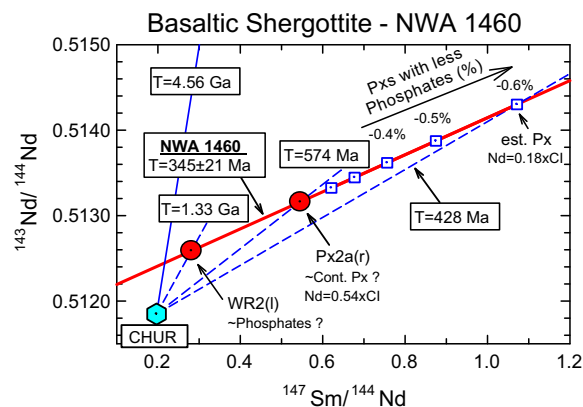


Fig. 9. Illustrating the effect of “correcting” the Sm–Nd isotopic systematics of NWA 1460 for a hypothetical admixture of “young” phosphate-borne Sm and Nd. Lacking reliable data from other mineral phases, a CHUR model age can be calculated to give the approximate time of elemental fractionation from an initially undifferentiated Mars. The solid (blue) line shows an absolute upper limit CHUR model age of 4.56 Ga. The dashed (blue) lines show various hypothetical CHUR model ages that can be constructed from the NWA 1460 data set. The oldest such model age of 1.33 Ga is obtained from the leachate data, for which the Sm–Nd isotopic data are dominated by those of phosphates. The crystallization age of NWA 1460 must be less than ~ 575 Ma as calculated for the uncorrected Px2a(r) analysis under the assumption that this sample contained some phosphate “contamination” (\sim Cont. Px?) because correcting for progressively larger amounts of hypothetical phosphate contamination results in progressively younger CHUR model ages. (For interpretation of the references to color in this figure legend, the reader is referred to the web version of this article.)

ages are not “unacceptably” old, i.e., >4.5 Ga. They interpret the melt pockets as having formed *in situ* during shock metamorphism, and imply that these melt pockets preferentially retained radiogenic ^{40}Ar when crystalline mineral phases were more severely degassed during shock metamorphism. However, the apparent ages of two melt pockets, Zagami #22 and NWA 1068 #22, are 4540 ± 18 Ma and 4440 ± 22 Ma, respectively, and thus are older than the 4050 ± 70 Ma Pb–Pb age preferred by Bouvier et al. (2008) as the crystallization age of shergottites. Moreover, Bogard and Park (2007, 2008b) pointed out that the ^{39}Ar – ^{40}Ar age spectrum of EET 79001,27 impact glass (a melt pocket in shergottite EET 79001) gives a relatively constant Ar–Ar age plateau of ~ 6 Ga, and thus cannot be a valid measure of the formation age of the impact-melted material. The high apparent age in EET 79001 impact glass occurs because of shock implantation of ^{40}Ar from the Martian atmosphere. Strong evidence that this excess ^{40}Ar is Martian atmosphere is the presence in the same impact glasses of other atmospheric species (^{36}Ar , Kr, Xe, N_2 , and CO_2) in approximately the proportions expected from the Viking measurements, and of isotopic fractionation of the $^{15}\text{N}/^{14}\text{N}$ and $^{36}\text{Ar}/^{38}\text{Ar}$ ratios due to atmospheric loss mechanisms (Bogard and Johnson, 1983; Wiens et al., 1986; Pepin and Carr, 1992; Marti et al., 1995; Bogard, 1997). The presence in many shergottites of

Ar from the Martian atmosphere as well as from the Martian interior (Bogard and Park, 2008) readily explains the observation that most shergottites give Ar–Ar ages older than ages obtained by other radiometric techniques.

In the case of Zagami, Bogard and Park (2008a) presented a strong argument against the hypothesis that shergottite ages were reset by shock metamorphism during ejection from the planet. Using a thermal model, and Ar–Ar ages and Ar diffusion data obtained from Zagami, these authors argued that a 4 Ga-old Zagami, shock-heated to a temperature of $\sim 70^\circ\text{C}$ (Fritz et al., 2005) at the time of Mars ejection ~ 3 Ma ago, could not have lost most of its ^{40}Ar by diffusion without having resided in space as an impossibly large body. Thus, Zagami's Ar–Ar age must record a formation age much younger than 4 Ga. An Arrhenius plot of Ar diffusion data for NWA 1460 (Bogard, 2009) shows that Ar diffusion in this shergottite is similar to that in Zagami and several other shergottites. Thus, the same thermal evaluation can be applied to Ar diffusion loss from NWA 1460. Using these diffusion data, the Ar–Ar age of NWA 1460, and the thermal model presented in Bogard and Park (2008a,b), NWA should have lost $\sim 97\%$ of the radiogenic ^{40}Ar present 350 Ma years ago. From the mineralogy and texture of NWA 1460, we estimate that it was shocked to no more than ~ 30 GPa and was not shock-heated above $\sim 300^\circ\text{C}$. Several other Martian meteorites shocked to ~ 30 GPa are estimated to have been heated to only $\sim 100^\circ\text{C}$ (Fritz et al., 2005). Applying this thermal model to NWA 1460, producing 97% ^{40}Ar loss by heating NWA 1460 to 300°C during Mars ejection would require its space radius to have been >1 km, clearly impossible values. Approximate space-ejected sizes of shergottites (see references and discussion in Park et al., 2008) are generally not more than a few tens of cm. If we assume the Mars-ejected radius of NWA 1460 to have been 30 cm, its shock heating temperature is required to significantly exceed 900°C . Only shergottite Dho 378 is known to have been shock-heated this high, and it shows significant shock melting and flow (Park et al., 2008). Even shock-heating NWA 1460 to 550°C would imply Mars ejection of a body ~ 10 – 100 m in radius, or $\sim 10^7$ – 10^{10} kg, which also is most unlikely.

With some modifications the arguments presented above can also be applied to the case of shock-metamorphism occurring on the Martian surface and depositing NWA 1460 into a thick ejecta layer to insulate the shocked material long enough for diffusion loss to occur. Furthermore, NWA 1460 shows no evidence of having been part of a large ejecta blanket. Barrat et al. (2002) concluded that paired shergottite NWA 480 formed from a melt in a single-stage, slow cooling event during which the pyroxenes grew continuously, and we make the same conclusion for NWA 1460. Thus, the only justifiable interpretation of the Ar–Ar age data of NWA 1460 plagioclase is that it and the concordant Sm–Nd and Rb–Sr ages represent the time when this diabasic rock crystallized from its parental magma.

Bouvier et al. (2008) argued that the $^{40}\text{Ar}/^{36}\text{Ar}$ ratio in the Martian atmosphere must always be less than that in the Martian mantle. Implicit in their argument is the

assumption that “the” mantle $^{40}\text{Ar}/^{36}\text{Ar}$ is determinable, presumably as a global average over different mantle reservoirs that may exist, in spite of the fact that ^{40}Ar and ^{36}Ar have different origins. The most precise determination of the recent Martian atmospheric ($^{40}\text{Ar}/^{36}\text{Ar}$)_{atm} is obtained from those impact glasses with high atmospheric gas content and low K concentrations. Perhaps the most precise determination of the atmospheric ($^{40}\text{Ar}/^{36}\text{Ar}$)_{atm} ratio is a value of ~ 1750 – 1900 reported by Garrison and Bogard (1998) for almost pure Martian atmospheric Ar in impact glass from EET 79001 and a few other shergottites, and similar values were obtained by Walton et al (2007). These ratios are lower than the $^{40}\text{Ar}/^{36}\text{Ar}$ ratio of 3000 ± 500 measured by the Viking Landers (Owen, 1976), and referenced by Bouvier et al. (2008). Considering the difficulty of the Viking measurements, the meteoritic determination of ($^{40}\text{Ar}/^{36}\text{Ar}$)_{atm} is preferred by most workers.

On elemental and isotopic ratio plots, most Martian gases define linear-like arrays that indicate variable mixing of Martian atmospheric and interior components. Many workers have attempted to characterize the Martian interior end-member compositions for various gases. Reported trapped ($^{40}\text{Ar}/^{36}\text{Ar}$)_{tr} ratios in shergottites range from <100 to almost 3000, all with large uncertainties. Most authors have attributed the lower ratios to a component from the Martian interior (e.g., Ott, 1988; Wiens and Pepin, 1988; Bogard and Garrison, 1998; Mathew and Marti, 2001; Schwenger et al., 2007; Walton et al., 2007). However, the Martian interior ($^{40}\text{Ar}/^{36}\text{Ar}$)_{MI} ratio remains poorly defined. From Ar–Ar analyses of mineral separates of Zagami and other shergottites, Bogard and Park (2008a,b) argued that the trapped interior ^{40}Ar concentrations in these samples are relatively constant and were inherited from the magma.

There are many factors that influence isotopic evolution of planetary volatiles such as the $^{40}\text{Ar}/^{36}\text{Ar}$ ratio, and differences in some of these factors between Mars and Earth account for different present compositions. To assert that the Martian atmospheric $^{40}\text{Ar}/^{36}\text{Ar}$ must be less than the mantle ratio (Bouvier et al., 2008) requires detailed consideration of all these factors, a task that may be beyond current ability. Here we only briefly summarize some factors that must be considered.

Compositional gradients of accreting material that formed the planets and uncertainties as to what fraction of planetary volatiles (e.g., Ar) accreted with the planets or was added later in volatile-rich material, raise the possibility that the K/ ^{36}Ar ratio (and thus average $^{40}\text{Ar}/^{36}\text{Ar}$) differs between Mars and Earth. Further, the tectonic and degassing history of the two planets obviously differ. Whereas plate tectonics on Earth has produced extensive melting of crust and mantle, Mars, without plate tectonics, probably melted very early, after which melting and mixing was limited. Because ^{36}Ar is an initial component, whereas ^{40}Ar forms slowly over time, such histories create local heterogeneities in the $^{40}\text{Ar}/^{36}\text{Ar}$ ratio. In our view, low and apparently variable values of trapped $^{40}\text{Ar}/^{36}\text{Ar}$ in the mantle source region of some shergottites, compared to the Martian atmospheric value, mean that there is substantial heterogeneity in $^{40}\text{Ar}/^{36}\text{Ar}$ among different Martian reservoirs. Even on a planet as active as the Earth, global

averaging of mantle $^{40}\text{Ar}/^{36}\text{Ar}$ appears to have been inefficient. As summarized by Allègre et al. (1986), mean $^{40}\text{Ar}/^{36}\text{Ar}$ values for mantle-derived rocks vary from ~ 390 for the Loihi seamount to $\sim 16,700$ for MORB. The mean value for the terrestrial continental crustal reservoir given by these authors is 20,600. Reservoirs contributing Ar of high $^{40}\text{Ar}/^{36}\text{Ar}$ ratio to the Martian atmosphere will be those characterized by high K abundances, and which outgas relatively late in the planet's history. For example, the Tharsis shield volcanoes are relatively young (cf. Werner, 2005, Fig. 15.13), and they and crustal regions to the south are characterized by relatively high K concentrations $> \sim 0.5$ wt.% (Taylor et al., 2007, Fig. 1). These values are significantly higher than the shergottite value of ~ 0.16 wt.% and also higher than the global Martian average. Thus, it seems likely that formation of the large Tharsis shield volcanoes contributed significantly to the ^{40}Ar inventory in the Martian atmosphere, and to a relatively high $^{40}\text{Ar}/^{36}\text{Ar}$ ratio, as has been argued by Phillips et al. (2001) for CO_2 , H_2O , and other volatiles.

The history of ^{36}Ar on Mars also is complex. Very early degassing into the atmosphere, followed by atmospheric loss likely occurred (Pepin (1991), and references therein). Decreased $^{36}\text{Ar}/^{38}\text{Ar}$ ratios in the current Mars atmosphere compared to Earth's atmosphere records a greater amount of ongoing fractionation loss for Mars (Jakosky et al., 1994). These factors would tend to increase atmospheric $^{40}\text{Ar}/^{36}\text{Ar}$ over time. Further, we note that the Martian atmospheric $^{129}\text{Xe}/^{132}\text{Xe}$ ratio of ~ 2.6 (Bogard et al., 2001) and the Martian interior ratio of ~ 1 , as determined in Martian meteorites (Ott, 1988), is just opposite from these atmospheric and interior ratios observed on Earth. Thus radiogenic ^{129}Xe , like radiogenic ^{40}Ar , is more concentrated in the Martian atmosphere than in the interior. Thus, we argue that relatively low "Martian Interior" $^{40}\text{Ar}/^{36}\text{Ar}$ values thus far derived from shergottites and other Martian meteorites should not be taken as an argument against young ages for shergottites because (a) in many cases the derived $^{40}\text{Ar}/^{36}\text{Ar}$ values are highly uncertain, (b) the planet's initial volatile inventory, outgassing history, atmospheric loss, and the characteristic Ar residence time(s) in different mantle source(s) are unknown factors, and (c) different and largely unsampled Martian mantle sources may have made highly variable contributions to the Martian atmospheric $^{40}\text{Ar}/^{36}\text{Ar}$ value.

6.2. Isotopic and trace element constraints on the petrogenesis of NWA 1460

6.2.1. REE patterns for NWA 1460/480 are similar to those for "Iherzolitic" shergottites

Barrat et al. (2002) reported major and trace element abundances in NWA 480, paired with NWA 1460. Fig. 10 compares Sm and Nd abundances in whole rock samples of both allocations of NWA 1460 to those in NWA 480 and confirms that the abundances are similar in the two specimens. Fig. 10 also compares chondrite-normalized REE abundances for NWA 480/1460 to those of four "Iherzolitic" shergottites, ALH 77005, LEW 88516, Yamato-793605, and Northwest Africa 1950, as well as to those

of EET 79001. The shapes of the REE patterns are similar for the "Iherzolitic" and NWA 480/1460 diabasic shergottites, but the latter are more enriched in the overall abundances of the REE. Although the heavy REE abundances in EET 79001 are nearly identical to those of NWA 480, the light REE abundances are $\sim 3\times$ lower. Primarily on the basis of the similarity of REE patterns, Barrat et al. (2002) suggested NWA 480/1460 and the "Iherzolitic" shergottites may have had similar parent liquids, or at least came from similar mantle sources. However, the ~ 346 Ma age of NWA 1460 is greater than the ~ 185 Ma age of "Iherzolitic" shergottites (Morikawa et al., 2001; Borg et al., 2002; Misawa et al., 2006), so these diabasic and "Iherzolitic" shergottites could not have shared the same parent liquid. Furthermore, the CRE ages of the two shergottite types are resolved, showing that they must have originated from different places on Mars. Consequently, we conclude that the similarity in their REE patterns is mantle-derived. EET 79001 is derived from a source region that has been more severely modified via earlier melt extractions that left it more depleted in LREE.

6.2.2. $^{87}\text{Sr}/^{86}\text{Sr}$ ingrowth for NWA 1460 and "Iherzolitic" shergottite sources: representative of bulk Mars?

Fig. 11 compares the age and initial $^{87}\text{Sr}/^{86}\text{Sr}$ of NWA 1460 to the ages and initial Sr isotopic compositions of the Iherzolitic shergottites ALH 77005 and LEW 88516, as well as to those of EET 79001 and to average nakhlite values. The dotted lines show the increase ("ingrowth") of $^{87}\text{Sr}/^{86}\text{Sr}$ with time in the Martian mantle in a simple two-stage model defined by (a) the mantle stage, and (b) the rock stage. In such models the variation of $^{87}\text{Sr}/^{86}\text{Sr}$ with time in the mantle is nearly linear because of the assumption that $^{87}\text{Rb}/^{86}\text{Sr}$ in the source region, $(^{87}\text{Rb}/^{86}\text{Sr})_s$, changes only as a result of radioactive decay of ^{87}Rb . The initial value of $(^{87}\text{Rb}/^{86}\text{Sr})_s$ is assumed to have been established during initial planetary differentiation near the beginning of the solar system, i.e., ~ 4.56 Ga ago. In reality, such two-stage models are almost certainly over-

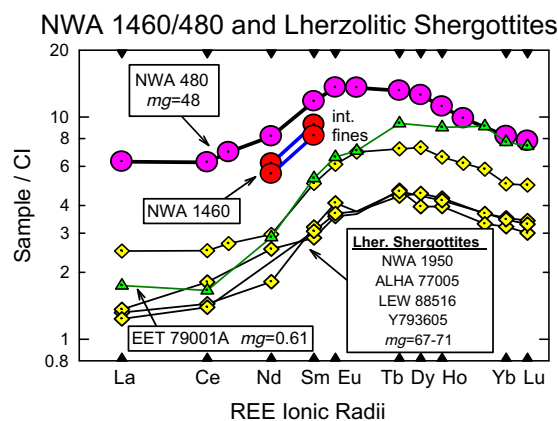


Fig. 10. Chondrite-normalized Sm and Nd abundances in NWA 1460 samples compared to those in NWA 480 (Barrat et al., 2002), EET79001 (Laul et al., 1986), and Iherzolitic shergottites. (LEW 88516: Dreibus et al., 1992; Yamato-793605: Warren and Kallemeyn, 1997; Northwest Africa 1950: Gillet et al., 2005).

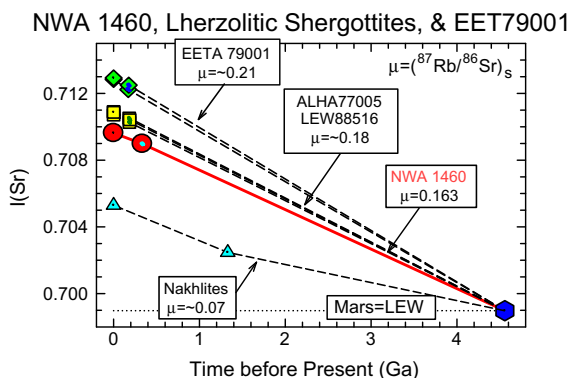


Fig. 11. Comparison of initial $^{87}\text{Sr}/^{86}\text{Sr}$ ingrowth for NWA 1460 (this investigation), lherzolithic shergottites (Shih et al., 1982; Borg et al., 2002), EET 79001 (Wooden et al., 1982; Nyquist et al., 2001c), and nakhlites (Shih et al., 2005, 2006) in two-stage models. Here $\mu = (^{87}\text{Rb}/^{86}\text{Sr})_S$ in Martian mantle source regions.

simplifications since they ignore, for example, changes in $(^{87}\text{Rb}/^{86}\text{Sr})_S$ caused by melt extractions prior to the formation times of the magmas in question. Nevertheless, they are useful in comparing the “time averaged” isotopic evolution in different magma sources.

Although the “lherzolithic” shergottites are younger than NWA 1460, the two-stage model calculations show that the time-averaged $(^{87}\text{Rb}/^{86}\text{Sr})_S$ ratios in the mantle sources of the two rock types (μ -values in Fig. 11) were very similar, differing by only $\sim 10\%$. A similar two-stage model shows that time-averaged $(^{87}\text{Rb}/^{86}\text{Sr})_S$ in the EET 79001 source was only $\sim 29\%$ higher than $(^{87}\text{Rb}/^{86}\text{Sr})_S = 0.163$ for the NWA 1460 source. The values of $(^{87}\text{Rb}/^{86}\text{Sr})_S$ for these rocks are remarkably close to one another when compared to the order of magnitude variation of two-stage model $(^{87}\text{Rb}/^{86}\text{Sr})_S$ values for SNC (shergottite–nakhlite–chassigny) meteorites from ~ -0.04 for depleted shergottites to ~ 0.35 for “enriched” shergottites.

Borg et al. (1997) estimated $(^{87}\text{Rb}/^{86}\text{Sr})_{\text{BSM}} \sim 0.16$ for Bulk Silicate Mars (BSM), a value identical to that given by the two-stage model for the NWA 1460 source. Shih et al. (1999) used a different geochemical approach to estimate $(^{87}\text{Rb}/^{86}\text{Sr})_{\text{BSM}} \sim 0.13$ for bulk Mars. Both of these estimates are similar to the two-stage model mantle values for NWA 1460 and the “lherzolithic” shergottites. Time averaged $(^{87}\text{Rb}/^{86}\text{Sr})_S$ for the nakhlites is lower than estimated for BSM by a factor of two. The isotopic systematics of the nakhlite source sometimes have been assumed to be representative of the Martian mantle (e.g., Jones, 1989; Longhi, 1991). Rb/Sr in this source appears to be approximately twofold lower than the BSM value, whereas Rb/Sr in NWA 1460 and the “lherzolithic” shergottites appears to be relatively undifferentiated from that of bulk Mars.

Fig. 11 shows very little difference between $(^{87}\text{Rb}/^{86}\text{Sr})_S$ calculated for NWA 1460’s mantle source, and measured bulk rock $(^{87}\text{Rb}/^{86}\text{Sr})_B = 0.123\text{--}0.131$ for NWA 1460 whole rock samples (Table 1). Although these present-day values are in excellent agreement with $(^{87}\text{Rb}/^{86}\text{Sr})_{\text{BSM}} \sim 0.13$ as estimated by Shih et al. (1999) for BSM, the Rb–Sr model ages of WRf1 and WR2 (Table 1) relative to $(^{87}\text{Sr}/^{86}\text{Sr})_{\text{LEW}} = 0.698972 \pm 8$ for the LEW86010 (“LEW”)

angrite (Nyquist et al., 1994) are ~ 5.9 Ga, and ~ 5.6 Ga, respectively, reflecting some lowering of $^{87}\text{Rb}/^{86}\text{Sr}$ in the mafic magma from the time-averaged value in the mantle of ~ 0.16 . This probably represents some preferential extraction of Rb relative to Sr in earlier partial melting events, leaving the mantle sources depleted in Rb. Nakhlites record the opposite behavior, i.e., $^{87}\text{Rb}/^{86}\text{Sr}$ in the rocks are significantly higher than the time-averaged value of ~ 0.07 in their mantle sources, suggesting either that Rb was preferentially extracted into the melt during partial melting, or that Sr had been preferentially extracted from the source in earlier melting events. For these shergottites, the close similarity in $^{87}\text{Rb}/^{86}\text{Sr}$ between time-averaged mantle values and present-day rock values suggests that the petrogenetic processes involved in their genesis did not significantly fractionate Rb/Sr ratios after the initial major fractionation arising from planetary differentiation.

6.2.3. $^{143}\text{Nd}/^{144}\text{Nd}$ ingrowth for NWA 1460 and “lherzolithic” shergottite sources

Fig. 12 is the Sm–Nd analog of Fig. 11 and compares the age and initial $^{143}\text{Nd}/^{144}\text{Nd}$ (expressed as ϵ_{Nd}) to the corresponding values for “lherzolithic” shergottites, EET 79001, and the nakhlites. This plot of ϵ_{Nd} vs. age shows that time-averaged Sm/Nd in the NWA 1460 source was similar to that in the source for “lherzolithic” shergottites. Thus, both the Rb–Sr and Sm–Nd isotopic data suggest similar

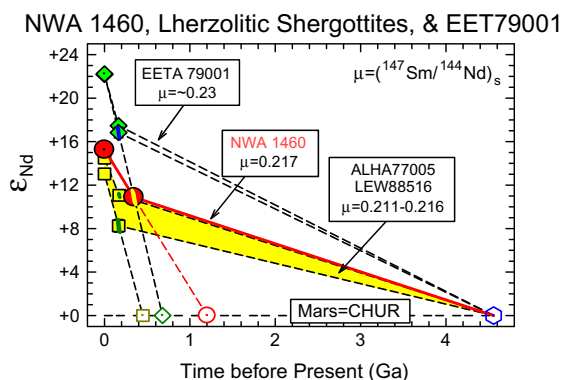


Fig. 12. Comparison of initial $^{143}\text{Nd}/^{144}\text{Nd}$ expressed as ϵ_{Nd} values (departure from chondritic Sm–Nd isotopic evolution in units of 10^4) for NWA 1460 (this investigation), lherzolithic shergottites (Shih et al., 1982; Borg et al., 2002a), EET 79001 (Wooden et al., 1982; Nyquist et al., 2001c), and nakhlites (Shih et al., 2005, 2006). Here $\mu = (^{147}\text{Sm}/^{144}\text{Nd})_S$ in Martian mantle source regions. NWA 1460 and the “lherzolithic” shergottites represent time-averaged Nd isotopic evolution that is closest to an undifferentiated chondritic value, and thus probably to Bulk Silicate Mars (BSM). The lowest $\mu = 0.211$ for LEW88516. Partial melts of the source region would yield magmas of decreased Sm/Nd ratios. Assuming Mars initially had a chondritic Sm/Nd ratio, melt extractions in the time interval of ~ 0.4 to ~ 1.2 Ga ago (open symbols) could lead to the observed values of initial ϵ_{Nd} for NWA1460. Convergence of ϵ_{Nd} ingrowth trajectories for “lherzolithic” sources, the NWA 1460 source, and backward extrapolation of the ingrowth rate in EET79001 suggests that the EET 79001 source could have been derived from the NWA1460 or “lherzolithic” shergottite source ~ 0.4 to ~ 0.6 Ga ago by melt extractions.

source regions for NWA 1460 and the “Iherzolitic” shergottites. However, as already noted for the Rb–Sr data, strictly two-stage models are unrealistic representations of the isotopic data. The Sm–Nd data show this effect in a more pronounced manner than the Rb/Sr data. That is, because the Sm/Nd ratio in the shergottite magma must have been *decreased* by partial melting of a more mafic mantle source, *the simple two-stage model cannot be correct in detail*. In the figure, the slopes of the evolution lines are proportional to the $(^{147}\text{Sm}/^{144}\text{Nd})_S$ values. Thus, immediately prior to the partial melting event the rate of radiogenic $^{143}\text{Nd}^*$ ingrowth in the source region must have been *greater* than in the mafic magma rather than less as implied by the two-stage model. Extrapolating the trajectory of $^{143}\text{Nd}/^{144}\text{Nd}$ ingrowth for NWA 1460 backward through its time of formation shows that it would reach the rate of growth in chondritic meteorites, i.e., the Chondritic Uniform Reservoir (CHUR) value, at ~ 1.2 Ga ago (open circle in Fig. 12). If the Martian mantle source of NWA 1460 were originally undifferentiated from CHUR, this T_{CHUR} value gives an approximation to the time when melt extractions began. The two-stage $(^{147}\text{Sm}/^{144}\text{Nd})_S \sim 0.217$ probably is an upper limit for $^{147}\text{Sm}/^{144}\text{Nd}$ in the NWA 1460 source over most of its history. $(^{147}\text{Sm}/^{144}\text{Nd})_S$ in the NWA 1460 source region is implied to have been close to that in the source of “Iherzolitic” shergottites, i.e., $(^{147}\text{Sm}/^{144}\text{Nd})_S \sim 0.211$ – 0.216 . Time averaged $(^{147}\text{Sm}/^{144}\text{Nd})_S$ ratios in both sources would have been relatively easily derived from the chondritic (CHUR) value of ~ 0.20 either during initial differentiation, or by later melt extractions in which Nd would have been preferentially removed. Evidence that the latter must have been a factor is provided by the observation that the $^{143}\text{Nd}/^{144}\text{Nd}$ ingrowth trajectory in the NWA source immediately prior to its formation must have been steeper than given by the two-stage model, i.e., there must have been prior melt extractions.

In contrast to the case for the shergottites, for nakhlites it is plausible to think of petrogenesis by partial melting of a source region with a two-stage model value of $(^{147}\text{Sm}/^{144}\text{Nd})_S = 0.235$ (not shown in Fig. 12), followed by partial melting during which the Sm/Nd ratio in the melt was significantly decreased relative to the source, causing the trajectory for $^{143}\text{Nd}/^{144}\text{Nd}$ ingrowth to evolve back towards $\epsilon_{\text{Nd}} = 0$, i.e., the CHUR value. Such a scenario has been modeled in detail by Shih et al. (2005).

The “Iherzolitic” shergottites have the lowest two-stage $^{147}\text{Sm}/^{144}\text{Nd}_S$ values among the shergottites that result in $\epsilon_{\text{Nd}} > \sim 0$, i.e., “mantle” values, and thus represent time-averaged Nd isotopic evolution that is closest to the undifferentiated chondritic value, i.e., closest to that of Bulk Silicate Mars (BSM). Indeed, Dreibus et al. (1992) noted on the basis of a large suite of major and trace element data that LEW 88516 (and ALH 77005) were “compositionally close to the Martian mantle”. Among the “Iherzolitic” shergottites, the lowest $^{147}\text{Sm}/^{144}\text{Nd}_S$ value is 0.211 for LEW88516. The higher $^{147}\text{Sm}/^{144}\text{Nd}_S$ values for the other “Iherzolitic” shergottites, as well as for NWA 1460 and EET 79001, may be the result of repeated melt extractions. Interestingly, the present-day $^{147}\text{Sm}/^{144}\text{Nd}$ ratio of EET 79001 could have been derived from the NWA 1460 or ALH 77005 sources at ~ 350 Ma ago because the evolution

lines for all three meteorites approximately converge at $\epsilon_{\text{Nd}} \sim 11$ then. Such a scenario is consistent with the greater light REE depletion of EET 79001 compared to NWA 1460 and the “Iherzolitic” shergottites (Fig. 10). A possible sequence of petrogenetic processes for these shergottites may have included: (a) initial differentiation of Mars and establishment of source regions with $(^{147}\text{Sm}/^{144}\text{Nd})_S$ near 0.1967, i.e., close to the CHUR value; (b) delayed magmatism starting only ~ 1.2 Ga ago; (c) periodic magma extractions during the interval ~ 1.2 to ~ 0.35 Ga ago; (d) extrusion of the NWA 1460 parental magma ~ 350 Ma ago; (e) continued magma extraction until ~ 175 Ma ago (EET79001).

6.2.4. Isotopic signatures of the Martian mantle sources of Martian meteorites

Fig. 13 summarizes the inferred isotopic signatures of the Martian mantle sources of Martian meteorites at 345 Ma ago. That is, ϵ_{Nd} is plotted vs. ϵ_{Sr} at 345 Ma ago assuming bulk Mars has a chondritic $^{147}\text{Sm}/^{144}\text{Nd}$ ratio and $^{87}\text{Rb}/^{86}\text{Sr} = 0.16$. With these assumptions, NWA 1460 and the “Iherzolitic” shergottites are close to bulk Mars in both parameters. The isotopic compositions of their sources likely were perturbed from BSM values by initial global differentiation followed by repeated melt extractions over geologic time, but they nevertheless appear to be our best representatives of the Nd and particularly the Sr isotopic characteristics of bulk Mars. Depleted shergottites and nakhlites have more pronounced mantle-type signatures with more positive ϵ_{Nd} and negative ϵ_{Sr} . The enrichment in ϵ_{Nd} for the depleted shergottites is greatest among the Martian meteorite suite, considerably greater than for the nakhlites, for example. However, depleted shergottites and nakhlites have similar ^{142}Nd enrichments (Debaille et al., 2007; Caro et al., 2008) showing that immediately following Martian global differentiation their mantle source regions had similar super-chondritic Sm/Nd ratios. This observation reinforces the suggestion that inter-

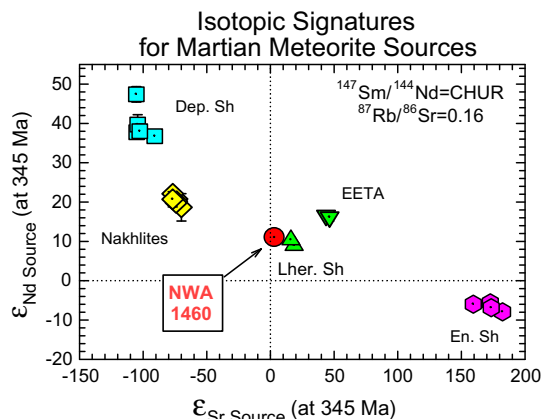


Fig. 13. Sr and Nd isotopic signatures of Martian mantle sources at 345 Ma ago. Data references for the “Iherzolitic” shergottites are given in Figs. 11 and 12 captions. Data references for depleted shergottites are Shih et al. (2005, 2007), and for “enriched” shergottites are Nyquist et al. (1995, 2000, 2001b).

mediate-to-late-stage melt extractions from the mantle sources of depleted shergottites caused radiogenic $^{143}\text{Nd}^*$ from decay of long-lived ^{147}Sm to grow in at an accelerated rate relative to its original growth rate, which would have been proportional to the ingrowth rate of radiogenic $^{142}\text{Nd}^*$ from decay of comparatively short-lived ^{146}Sm . It seems likely that the mantle sources of the nakhlites remained approximately closed between the original Martian differentiation event and melt extractions ~ 1.3 Ga ago.

In the representation of Fig. 13, the “enriched” shergottites show “crustal” signatures with negative ε_{Nd} and positive ε_{Sr} . It is unclear, however, whether this signature arises from assimilation of crustal material (Jones, 1986; Rumble and Irving, 2009), or reflects the influence of residual liquid from the Martian global differentiation that became trapped in the mantle during late-stage mantle overturn (Borg and Draper, 2003; Elkins-Tanton et al., 2003). In either hypothesis, the isotopic compositions of the “enriched” shergottites would not represent true mantle values.

6.3. Northwest Africa 1460 in Martian context

6.3.1. Probable provenance of NWA 1460

As for all Martian meteorites, complete interpretation of the chronology and isotopic data for NWA 1460 is hampered by lack of knowledge of the geology of the terrain from which it came. It is difficult even to achieve consensus on the number of different Martian “sampling” events which the meteorites represent. One approach has been to plot crystallization age against “ejection” age as in Nyquist et al. (2001a). This approach assumes that impact events occur on unique surfaces with unique ages, and at uniquely defined times. Other authors have assumed that surface rocks of multiple ages may be sampled by a single event, and prefer to define the number of ejection events from ejection ages only (e.g., Christen et al., 2005). NWA 1460 and 480 have similar crystallization and ejection ages (Mathew et al., 2003; Nishiizumi et al., 2004; Connolly et al., 2006; Nishiizumi and Caffee, 2006) to those of depleted shergottite QUE 94201, and these specimens also have very similar ejection ages to those of many “enriched” shergottites, including Zagami.

Using both crystallization age and ejection age as discriminators, Nyquist et al. (2001a, Fig. 8) concluded that the number of individual ejection events lay in the range 4–8. With the same criteria, it is possible to count nine individual ejection events from the current data. Three of these events are unambiguously defined, and may be designated “O” (orthopyroxenite ALH84001), “NC” (nakhlites and chassignites), and “S_{Dho}” (Dhofar 019). The situation for the remaining shergottites is more ambiguous. In approximate order of increasing apparent ejection age (cf. Christen et al., 2005, Fig. 1), one can count S_E (EET 79001: ejection age ~ 0.7 Ma, crystallization age ~ 175 Ma), S_{DYN} (DaG 476, Y-980459, NWA 1195: ejection age ~ 1.25 Ma, crystallization age ~ 475 Ma except for NWA 1195 with a crystallization age of ~ 347 Ma (Symes et al., 2008), S_Z (the main “enriched” shergottite group including Zagami and Shergotty: ejection age ~ 2.8 Ma, crystallization age ~ 165 – 175 Ma), S_Q (NWA 1460/480 and QUE94201: ejection

age ~ 2.5 Ma, crystallization age ~ 325 – 350 Ma), S_L (“Iherzolitic” shergottites: ejection age ~ 4 Ma, crystallization age ~ 185 Ma), and S₆₈ (NWA 1068: ejection age ~ 1.25 Ma, crystallization age ~ 165 Ma).

Crater-frequency ages $< \sim 1$ Ga have been reported recently for a few Martian surfaces (Neukum et al., 2004; Werner, 2005; Neukum et al., 2007). Most surfaces with cratering model ages similar to those of the Martian meteorites are located on the flanks or within the calderas of the Tharsis volcanoes (Alba Patera, Olympus Mons, Arsia Mons, Pavonis Mons, and Ascaeus Mons), or Hecatus Tholus on the Elysium plains. In two instances, Kasei Valles adjacent to Chryse Planitia, and Mangalla Valles adjacent to Amazonis Planitia, fluvial channels from the highlands flow onto young volcanic surfaces, leading to the suggestion that the fluvial activity was triggered by the adjacent volcanic activity (cf. Werner, 2005, Fig. 14.11). The probability for seven shergottite-ejecting impacts on these eight identified young surfaces is low.

Neukum et al. (2004) argued that there need not be a direct genetic relationship between the known young Martian surfaces and the Martian meteorite ages, but that the observations suggest Martian volcanic activity was probably episodic in nature, generating large surface units at preferred times, some of which are recorded in the Martian meteorites. Nevertheless, assuming the validity of the cratering model ages, the possibility that the number of separate shergottite ejection events has been over-counted needs to be considered. Meteorites of differing crystallization ages may be sampled in a single ejection event due to local stratigraphy. Pre-exposure on the Martian surface to the effects of cosmic-ray interactions could lead to CRE ages in excess of the true ejection age. For example, the “enriched” shergottites like Zagami share a common crystallization age with “Iherzolitic” shergottites and EET 79001, suggestive of a common event. That would require pre-exposure of some of the “Iherzolitic” shergottites, and in-space breakup for EET 79001, but would reduce the number of shergottite ejection events by two.

Hitherto secondary break-up has been considered unlikely (e.g., Bogard et al., 1984; Warren, 1994), but Popova et al. (2007), conclude that in space some bolides consist of highly fractured “swarms” traveling as a single mass, as shown by progressive fragmentation as they enter a planetary atmosphere, as evidenced by clusters of closely associated craters. For “small clusters” of craters with diameters of tens of meters spread over a region of a few hundred meters, Popova et al. (2007) infer that the parent meteoroid masses were fractured during prior asteroid collisions. They conclude that “large clusters” of craters of diameter a few hundred meters spread over a region of ~ 2 – 30 km are secondary craters from a primary impact, and that large blocks of ejecta were fragmented not only during descent, but also during *ascent*, i.e., that large, initially fragmented blocks were launched. They concluded that these larger clusters probably were associated with primary craters of diameter ~ 15 to $> \sim 85$ km.

To explain the large clusters as secondary craters, Popova et al. (2007) require launch of blocks on the order of five meters to a few hundred meters on a side at velocities

of $\sim 3\text{--}5$ km/s. For comparison, their favored scenario for Martian meteorites is launch from craters $>3\text{--}7$ km in diameter (Head et al., 2002) “somewhat favoring the larger sizes”. This size limit thus approaches the lower limit they consider for large cluster production by ejected blocks >5 m in size. If highly fragmented blocks large enough to provide shielding to cosmic ray interaction for interior samples (i.e., ~ 2 m in diameter) were launched from Mars, the possibility that a close gravitational encounter during aphelion passage through the asteroid belt (cf. Nyquist et al., 2001a,b,c) could cause disruption and exposure of previously shielded interior material needs to be considered. Such a scenario is of no interest for most of the Martian meteorites for which cosmogenic nuclide data suggest ejection from Mars as small objects, but may be of interest for EET 79001 for which the crystallization age of 174 ± 3 Ma (Nyquist et al., 2001b) matches exactly those of several “enriched” shergottites, but for which the ejection age of ~ 0.7 Ma is fourfold lower than that of the “enriched” shergottites (cf. Christen et al., 2005). Interestingly, the observed variation of cosmogenic $(^{21}\text{Ne}/^{22}\text{Ne})_{\text{cos}}$ for subsamples of EET 79001 is the greatest among the shergottites, including, in particular, some values larger than for the other shergottites (Schwenzer et al., 2007). Larger values of $(^{21}\text{Ne}/^{22}\text{Ne})_{\text{cos}}$ imply greater shielding. The range of $(^{21}\text{Ne}/^{22}\text{Ne})_{\text{cos}}$ for EET 79001 as summarized by Schwenzer et al. (2007, Fig. 5) greatly exceeds the range of possible ratios calculated for galactic cosmic ray spallation according to the production rates of Leya et al. (2000) for meteoroid radii up to 85 cm (high mass, high $^{21}\text{Ne}/^{22}\text{Ne}$ end) with three data points exceeding the calculated “maximum” value. Schwenzer et al. (2007) attribute such data to mineralogical variability and fortuitous measurements of pieces with unusual composition, but perhaps EET 79001 does not represent a separate ejection event, but instead experienced a complex exposure history with part of that exposure in a body >85 cm in radius. (Unusually low values of $(^{21}\text{Ne}/^{22}\text{Ne})_{\text{cos}}$ for most of the EE79001 data compared to the calculated range are attributed by Schwenzer et al. (2007) to the action of solar cosmic rays, but this is not the explanation for high $(^{21}\text{Ne}/^{22}\text{Ne})_{\text{cos}}$.) Further, one might consider the possibility that “lherzolitic” shergottites with ejection ages only $\sim 30\%$ older than those of the more common “enriched” basaltic shergottites of similar crystallization age (cf. Christen et al., 2005) were exposed to cosmic rays on the Martian surface prior to their ejection. Uncertainties in the CRE ages arise from variations in the production rates of cosmogenic nuclides in meteorites due to differing chemical compositions as well as differing degrees of shielding within the parent meteoroid. For example, highly variable CRE ages calculated for the olivine-phyric shergottite NWA 1068 are likely caused by uncertainties in matching production rates to chemical composition. With respect to trace element and isotopic characteristics, NWA 1068 is an “enriched” shergottite, and among its CRE ages cited by Christen et al. (2005) the ^{15}N age of 2.6 Ma is a close match to those of other “enriched” shergottites. Further, if S_Q and S_Z for similar ejection ages, but different rock ages are accepted as a single event, the number of Amazonian ejection events might be reduced

to a minimum of three, and the total number of ejection events reduced to a minimum of five.

An advantage claimed for the hypothesis of the Lyon group (Bouvier et al., 2005, 2008) is that it would reduce the required number of meteorite ejection events from Amazonian terrain to only one, the NC event. However, this hypothesis would then require multiple ejection events from heavily cratered, fractured, and weathered Noachian terrain. Current theories and simulations of the meteorite ejection process show that ejection from coherent, mechanically strong surfaces is strongly favored (cf. Hartmann and Barlow, 2006). Thus, the Lyon hypothesis cannot be reliably invoked to explain the apparent over-abundance of young rocks in the Martian meteorite population compared to the ages of the Martian surfaces from which they were ejected (cf. Treiman, 1995; Nyquist et al., 1998).

6.3.2. Do Martian meteorite ages support current crater frequency model ages?

Significant uncertainty appears to remain in the absolute age calibration of the Martian cumulative crater frequency curve. Fig. 14 summarizes Martian meteorite crystallization ages compared to (i) the Neukum et al. (2001) cumulative crater frequency curve for craters >1 km in diameter on the moon, a basic reference for cratering model ages, (ii) the derivative Martian cumulative crater frequency curves for craters >1 km on Mars, as given by Werner (2005), (iii) a curve fit to lunar cumulative crater frequencies as summarized by Stöffler and Ryder (2001) and multiplied by a Mars/Moon crater production ratio of 1.55 for craters having diameters of 2–50 km (Hartmann, 2005). The “Stöffler & Ryder” curve illustrated in Fig. 14 is fit to data presented in Fig. 11 of Stöffler and Ryder (2001), including the age and crater frequency parameters given in their Table VI for the crater Copernicus. Neukum et al. (2001) ignore the Copernicus datum, preferring instead an essentially constant cratering rate between ~ 3.0 Ga ago and the present, as shown in their Fig. 10. Fig. 14 also illustrates the probable location of the crater frequency/age data for the crater Autolycus (Ryder et al., 1991; Stöffler and Ryder, 2001) and a suggested value for the crater Aristillus (Ryder et al., 1991).

Fig. 14 also shows the cumulative crater frequency per km^2 for craters >1 km diameter ($N_{\text{cum}}(1 \text{ km})$; Werner, 2005) for “Amazonis unit 2 north” (Werner, 2005; Table 14.1). This is unit AAa2n of Tanaka et al. (2005) and has a cratering model age of 1.1–1.45 Ga as derived by Werner (2005) and illustrated in Fig. 14 at the intersection of the “Werner (2005)” curve and the tabulated crater frequency of $(5.3\text{--}7.1) \times 10^{-4} \text{ km}^{-2}$. The same crater frequency would correspond to younger ages of ~ 0.75 Ga for the Neukum et al. (2001) curve, i.e., for a Mars/Moon cratering ratio of 1.0, and to an even younger age of ~ 0.5 Ga for the Stöffler & Ryder lunar curve. The latter value is equivalent to the ages of the oldest shergottites, thus making unit AAa2n a candidate source area for ejection events of the older shergottites. Fig. 14 also illustrates adjustment of the Stöffler & Ryder lunar curve by a Mars/Moon ratio of 1.55 as derived from Hartmann (2005) for craters in the size range 2–50 km in diameter. This adjustment places the NC event and the

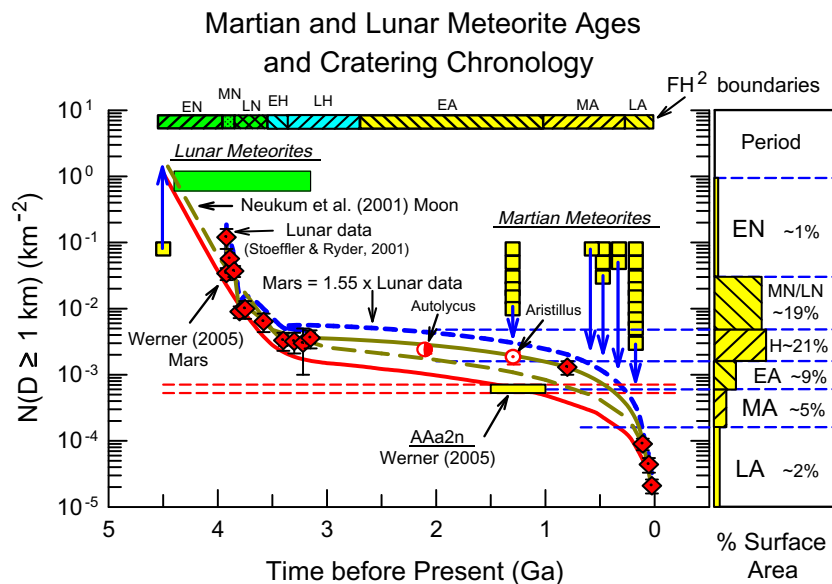


Fig. 14. Martian meteorite crystallization ages compared to: (i) the Neukum et al. (2001) cumulative crater frequency curve for craters >1 km in diameter ($N(D > 1 \text{ km})$ per km^2 on the moon); (ii) the derivative Martian cumulative crater frequency curves for craters >1 km on Mars, as given by Werner (2005); (iii) period boundaries for the Tanaka (1986) cratering periods from Fassett and Head (2008) using the Hartmann system (FH^2 , top); (iv) a curve fit to lunar cumulative crater frequencies as summarized by Stöffler and Ryder (2001); (v) the same curve multiplied by a Mars/Moon crater production ratio of 1.55 for craters having diameters of 2–50 km (Hartmann, 2005). The right hand axis shows the percent surface area of volcanics calculated from Tanaka et al. (1992, Table V) for period boundaries for $N(D > 1 \text{ km})/\text{km}^2$ taken from Werner (2005, Fig. 5.1). Also shown are crater counts from “Amazonis unit 2 north” (Werner, 2005), i.e., unit AAa2n of Tanaka et al. (2005).

earlier shergottite events (S_{Dho} , S_{DYN}) into the Hesperian cratering epoch (Tanaka, 1986), and younger, 175–346 Ma events into the Early Amazonian. The fraction of the total Martian volcanic surface areas in the Hesperian and Early Amazonian is significant, $\sim 30\%$ *in toto*. This readjustment of the Martian cratering curve dramatically improves the relative probability of ejection of meteorites with ages within the observed age spectrum compared to meteorites of older ages.

An ambiguous role for secondary cratering introduces an additional uncertainty into cratering chronology studies for young Martian surfaces. For example, McEwen et al. (2005) concluded that 80% of the impact craters superposed on the youngest surfaces in the Cerberus plains were related to the single 10-km rayed crater Zunil in the Cerberus Plains of Elysium Planitia. Indeed, McEwen et al. (2005) suggest that the crater Zunil is a plausible source crater for basaltic shergottites with emplacement ages of ~ 170 Ma and ejection ages of ~ 2.7 Ma (our S_Z event for “enriched” shergottites). Whether or not Zunil crater is the source crater for the “enriched” shergottites, it appears that there are parts of the Cerberus Plains of appropriate age (Lanagan and McEwen, 2003) to host an ejection crater for the ~ 165 – 175 Ma “enriched” shergottites (McEwen et al., 2005).

7. CONCLUSIONS

Multiple lines of evidence show that the Rb–Sr, Sm–Nd, and Ar–Ar ages of Northwest Africa 1460 individu-

ally give robust crystallization ages for this basaltic (or diabasic) shergottite. Thus, there can be little doubt that these concordant ages of NWA 1460 define its crystallization age to be ~ 346 Ma. The arguments advanced by Bouvier et al. (2008) to explain why shergottite ages obtained by these three radiometric techniques are much less than the presumptive primary formation age of ~ 4 Ga preferred by these authors do not apply to NWA 1460. Moreover, Martian meteorite ages can now be plausibly understood within the broader context of Martian geology and the “shergottite age paradox” (Nyquist et al., 1998) is lessened. The alternative interpretation that the shergottites are really ~ 4.1 Ga old (Bouvier et al., 2005, 2008) provides no practical advantage in this regard. Indeed, it encounters the disadvantage that launch of meteorites from ~ 4.0 Ga terrain appears to be strongly discriminated against (cf. Hartmann and Barlow, 2006). Furthermore, any such ancient rocks, if launched, presumably would show much more evidence of alteration than is shown by the pristine shergottite meteorites. This expectation follows from examination of the rocks at Gusev Crater by the Spirit Mars Exploration Rover, for example.

Currently emerging cratering model ages have identified a number of candidate source areas on Mars of appropriate apparent ages to be the source terrains for Martian meteorites. However, current cratering models need direct calibration via radiometric age determination of Martian rocks before the cratering model ages can be taken as definitive. The Martian meteorite ages suggest

that the current models are likely to be revised with respect both to the relative Mars/Moon cratering ratio, and also with respect to the time dependence of cratering rates at relatively young ages. The first task would be most reliably achieved with a properly chosen returned Martian sample, but we agree with Stöfler and Ryder (2001) that analysis of returned lunar samples from terrains of Eratosthenian and Copernican age also would greatly improve our understanding of the lunar reference curve at young ages.

Finally, we argue that the intermediate initial Sr- and Nd-isotopic composition of NWA 1460 identifies this basaltic shergottite (and paired stone NWA 480) and the “Iherzolitic” shergottites as giving the best current approximation to the Sr- and Nd-isotopic composition of bulk silicate Mars. These isotopic compositions are not the result of simple two-stage mantle/melt evolution, but likely result from multiple melt extractions from individual locations in the Martian mantle extending to relatively recent times, i.e., within the past ~1 Ga.

ACKNOWLEDGMENTS

The specimens used for this study were generously provided by Nelson Oakes. Constructive comments by Dimitri Papanastassiou and two anonymous reviewers as well as by Associate Editor Greg Herzog hopefully resulted in significant improvement of an earlier version of the manuscript. Financial support was provided by the NASA Cosmochemistry Program. J.P. was supported by a NASA Postdoctoral Program fellowship.

APPENDIX A

See Table A1.

Table A1

The ^{39}Ar – ^{40}Ar isotopic data for shergottite NWA 1460. Columns from left to right give extraction temperature, ^{39}Ar concentration, Age, K/Ca ratio, and Ar isotopic ratios. Uncertainties in age, K/Ca, and isotopic ratios are given beside each value.

Temperature (°C)	^{39}Ar (10^{-9}) $\text{cm}^3\text{STP/g}$	Age (Ma)	K/Ca ratio	$^{40}\text{Ar}/^{39}\text{Ar}$	$^{38}\text{Ar}/^{39}\text{Ar}$	$^{37}\text{Ar}/^{39}\text{Ar}$	$^{36}\text{Ar}/^{39}\text{Ar}$
300	1.81	962.3 ± 45.8	0.786 ± 0.053	33.38 ± 2.04	0.782 ± 0.067	0.70 ± 0.05	0.0766 ± 0.0116
400	2.30	672.9 ± 41.7	0.420 ± 0.033	21.42 ± 1.59	0.513 ± 0.053	1.31 ± 0.10	0.0675 ± 0.0103
500	10.46	329.8 ± 11.6	0.548 ± 0.023	9.50 ± 0.36	0.304 ± 0.017	1.00 ± 0.04	0.0317 ± 0.0027
600	11.26	466.2 ± 15.1	0.084 ± 0.003	13.97 ± 0.51	0.460 ± 0.024	6.58 ± 0.26	0.0135 ± 0.0019
650	12.13	583.1 ± 19.6	0.087 ± 0.004	18.07 ± 0.71	0.408 ± 0.023	6.33 ± 0.27	0.0257 ± 0.0023
750	37.18	512.3 ± 31.0	0.048 ± 0.004	15.56 ± 1.08	0.839 ± 0.082	11.49 ± 0.85	0.0140 ± 0.0017
780	25.82	442.2 ± 10.3	0.051 ± 0.001	13.16 ± 0.34	0.462 ± 0.017	10.82 ± 0.32	0.0104 ± 0.0010
810	24.22	411.4 ± 11.0	0.052 ± 0.002	12.13 ± 0.36	0.405 ± 0.017	10.48 ± 0.35	0.0089 ± 0.0009
840	21.83	413.2 ± 12.2	0.051 ± 0.002	12.19 ± 0.40	0.492 ± 0.023	10.72 ± 0.39	0.0088 ± 0.0010
870	23.52	401.1 ± 11.4	0.049 ± 0.002	11.79 ± 0.37	0.508 ± 0.023	11.31 ± 0.39	0.0107 ± 0.0010
900	30.79	367.7 ± 9.0	0.048 ± 0.001	10.71 ± 0.29	0.405 ± 0.016	11.53 ± 0.35	0.0093 ± 0.0008
930	35.00	350.5 ± 8.0	0.046 ± 0.001	10.16 ± 0.25	0.410 ± 0.015	12.05 ± 0.34	0.0088 ± 0.0008
960	43.17	360.7 ± 6.6	0.043 ± 0.001	10.48 ± 0.21	0.469 ± 0.013	12.76 ± 0.30	0.0082 ± 0.0007
990	37.07	360.0 ± 7.6	0.041 ± 0.001	10.46 ± 0.24	0.432 ± 0.014	13.39 ± 0.35	0.0079 ± 0.0007
1030	27.65	358.1 ± 10.0	0.038 ± 0.001	10.40 ± 0.32	0.427 ± 0.019	14.36 ± 0.48	0.0090 ± 0.0009
1100	41.39	363.6 ± 6.8	0.041 ± 0.001	10.58 ± 0.22	0.349 ± 0.008	13.57 ± 0.32	0.0091 ± 0.0006
1200	16.56	363.4 ± 15.9	0.047 ± 0.002	10.57 ± 0.51	0.304 ± 0.016	11.64 ± 0.60	0.0112 ± 0.0009
1300	6.33	393.6 ± 31.1	0.046 ± 0.004	11.55 ± 1.01	0.362 ± 0.045	11.90 ± 1.11	0.0032 ± 0.0015
1400	2.92	736.7 ± 55.7	0.049 ± 0.005	23.89 ± 2.20	0.307 ± 0.032	11.34 ± 1.11	0.0627 ± 0.0077

REFERENCES

- Allègre C. J., Staudacher T. and Sarda P. (1986) Rare gas systematics: formation of the atmosphere, evolution and structure of the Earth's mantle. *Earth Planet. Sci. Lett.* **81**, 127–150.
- Aramovich C. J., Herd C. D. K. and Papike J. J. (2002) Symplectites derived from metastable phases in Martian basaltic meteorites. *Am. Mineral.* **87**, 1351–1359.
- Barrat J. A., Gillet Ph., Sautter V., Jambon A., Javoy M., Göpel C., LeSourd M., Keller F. and Petit E. (2002) Petrology and chemistry of the basaltic shergottite North West Africa 480. *Meteorit. Planet. Sci.* **37**, 487–499.
- Beck P., Ferroir T., Gillet P., Montagnac G., Bohn M. and Lesourd M. (2006) Shock melting of Martian basalts and the entrapment of atmospheric gases. *Lunar Planet. Sci. XXXVII*. Lunar Planet. Inst., Houston. #1939 (abstr.).
- Blundy J. D. and Wood B. J. (1991) Crystal chemical control of partitioning of Sr and Ba between plagioclase feldspar, silicate melts, and hydrothermal solutions. *Geochim. Cosmochim. Acta* **55**, 193–209.
- Bogard D. D. (1997) A reappraisal of the Martian $^{36}\text{Ar}/^{38}\text{Ar}$ ratio. *J. Geophys. Res. Planets* **102**(E1), 1653–1661.
- Bogard D. D. (2009) K–Ar dating of rocks on Mars: requirements from Martian meteorite analyses and isochron modeling. *Meteorit. Planet. Sci.* **44**, 3–14.
- Bogard D. D. and Johnson P. (1983) Martian gases in an Antarctic meteorite? *Science* **221**, 651–654.
- Bogard D. D. and Garrison D. H. (1998) Relative abundances of argon, krypton, and xenon in the Martian atmosphere as measured in Martian meteorites. *Geochim. Cosmochim. Acta* **62**, 1829–1835.
- Bogard D. D. and Park J. (2007) Ar–Ar age of NWA-1460 and evidence for young formation ages of the shergottites. *Lunar Planet. Sci. XXXVIII*. Lunar Planet. Inst., Houston. #1096 (abstr.).
- Bogard D. D. and Garrison D. H. (2008) ^{39}Ar – ^{40}Ar age, thermal history of Martian dunite NWA 2737. *Earth Planet. Sci. Lett.* **273**, 386–392.

- Bogard D. D. and Park J. (2008a) ^{39}Ar - ^{40}Ar dating of the zagami Martian shergottite and implications for magma origin of excess ^{40}Ar . *Meteorit. Planet. Sci.* **43**, 1113–1126.
- Bogard D. D. and Park J. (2008b) Excess ^{40}Ar in Martian shergottites, K- ^{40}Ar ages of nakhlites, and implications for *in situ* K-Ar dating of Mars' surface rocks. *Lunar Planet. Sci. XXXIV*. Lunar Planet. Inst., Houston. #1100 (abstr.).
- Bogard D. D., Nyquist L. E. and Johnson P. (1984) Noble gas contents of shergottites and implications for the Martin origin of SNC meteorites. *Geochim. Cosmochim. Acta* **48**, 1723–1739.
- Bogard D. D., Garrison D. H., Norman M., Scott E. R. D. and Keil K. (1995) ^{39}Ar - ^{40}Ar age and petrology of Chico: large-scale impact melting of the L chondrite parent body. *Geochim. Cosmochim. Acta* **59**, 1383–1400.
- Bogard D. D., Clayton R. N., Marti K., Owen T. and Turner G. (2001) Martian volatiles: isotopic composition, origin, and evolution. *Space Sci. Rev.* **96**, 427–457.
- Borg L. E. and Draper D. S. (2003) A petrological model for the origin and compositional variations of the Martian basaltic meteorites. *Meteorit. Planet. Sci.* **38**, 1713–1732.
- Borg L. E., Nyquist L. E., Taylor L. A., Wiesmann H. and Shih C.-Y. (1997) Constraints on Martian differentiation processes from Rb-Sr and Sm-Nd isotopic analyses of the basaltic shergottite QUE94201. *Geochim. Cosmochim. Acta* **61**, 4915–4931.
- Borg L. E., Nyquist L. E., Wiesmann H. and Reese Y. (2002) Constraints on the petrogenesis of Martian meteorites from the Rb-Sr and Sm-Nd isotopic systematics of the Iherzolitic shergottites ALH77005 and LEW88516. *Geochim. Cosmochim. Acta* **66**, 2037–2053.
- Botte W. F., Vokrouhlicky D. and Nesvorny D. (2007) An asteroid breakup 160 Myr ago as the probable source of the K/T impactor. *Nature* **449**, 48–53.
- Bouvier A., Blichert-Toft J., Vervoort J. D. and Albarède F. (2005) The age of SNC meteorites and the antiquity of the Martian surface. *Earth Planet. Sci. Lett.* **240**, 221–233.
- Bouvier A., Blichert-Toft J., Vervoort J. D., Gillet P. and Albarède F. (2008) The case for old basaltic shergottites. *Earth Planet. Sci. Lett.* **266**, 105–124.
- Caro G., Bourdon B., Halliday A. N. and Quitte G. (2008) Superchondritic Sm/Nd ratios in Mars, the Earth and the Moon. *Nature* **452**, 336–339.
- Christen F., Eugster O. and Busemann H. (2005) Mars ejection times and neutron capture events of the nakhlites Y000593 and Y000749, the olivine-phyric shergottite Y980459, and the Iherzolite NWA1950. *Antarct. Meteorit. Res.* **18**, 117–132.
- Connolly, Jr., H. C., Zipfel J., Grossman J. N., Folco L., Smith C., Jones R. H., Righter K., Zolensky M., Russell S. S., Benedix G. K., Yamaguchi A. and Cohen B. A. (2006) The meteoritical bulletin, No. 90. *Meteorit. Planet. Sci.* **41**, 1383–1418.
- Debaille V., Brandon A. D., Yin Q. Z. and Jacobsen B. (2007) Coupled ^{142}Nd - ^{143}Nd evidence for a protracted magma ocean in Mars. *Nature* **450**, 525–528.
- Dreibus G., Jochum K. H., Palme H., Spettel B., Wlotzka F. and Wänke H. (1992) LEW88516: a meteorite compositionally close to the “Martian mantle” (abstr.). *Meteoritics* **27**, 216–217.
- Elkins-Tanton L. T., Parentier E. M. and Hess P. C. (2003) Magma ocean fractional crystallization and cumulate overturn in terrestrial planets: implications for Mars. *Meteorit. Planet. Sci.* **38**, 1753–1772.
- Eugster O., Weigel A. and Polnau E. (1997) Ejection times of Martian meteorites. *Geochim. Cosmochim. Acta* **61**, 2749–2757.
- Eugster O., Busemann H., And Lorenzetti S. and Terribilini D. (2002) Ejection ages from ^{81}Kr -Kr dating and pre-atmospheric sizes of Martian meteorites. *Meteorit. Planet. Sci.* **37**, 1345–1360.
- Fassett C. I. and Head J. W. (2008) The timing of Martian valley network activity: constraints from buffered crater counting. *Icarus* **195**, 61–89.
- Fritz J., Artemieva N. and Greshake A. (2005) Ejection of Martian meteorites. *Meteorit. Planet. Sci.* **40**, 1393–1411.
- Garrison D. H. and Bogard D. D. (1998) Isotopic composition of trapped and cosmogenic noble gases in several Martian meteorites. *Meteorit. Planet. Sci.* **33**, 721–736.
- Garrison D., Hamlin S. and Bogard D. (2000) Chlorine abundances in meteorites. *Meteorit. Planet. Sci.* **35**, 419–429.
- Gillet P., Barrat J. A., Beck P., Marty B., Greenwood R. C., Franchi I. A., Bohn M. and Cotton J. (2005) Petrology, geochemistry and cosmic-ray exposure age of Iherzolitic shergottite Northwest Africa 1950. *Meteorit. Planet. Sci.* **40**, 1175–1184.
- Hartmann W. K. (2005) Martian cratering 8: isochron refinement and the chronology of Mars. *Icarus* **174**, 294–320.
- Hartmann W. K. and Barlow N. (2006) Nature of Martian uplands: effect on Martian meteorite age distribution and secondary cratering. *Meteorit. Planet. Sci.* **41**, 1453–1468.
- Head J. N., Melosh H. J. and Ivanov B. A. (2002) Martian meteorite launch: high-speed ejecta from small craters. *Science* **298**, 1752–1756.
- Herd C. D. K., Simonetti A. and Peterson N. D. (2007) *In situ* U-Pb geochronology of Martian baddeleyite by laser ablation MC-ICPMS. *Lunar Planet. Sci. XXXVIII*. Lunar Planet. Inst., Houston. #1664 (abstr.).
- Ikeda Y., Kimura M., Takeda H., Shimoda G., Kita N. T., Morishita Y., Suzuki A., Jagoutz E. and Dreibus G. (2006) Petrology of a new basaltic shergottite: Dhofar 378. *Antarct. Meteorit. Res.* **19**, 20–44.
- Irving A. J. and Kuehner S. M. (2003) Petrology of NWA 1460: a baddeleyite-bearing shergottite paired with NWA 480. *Lunar Planet. Sci. XXXIV*. Lunar Planet. Inst., Houston. #1503 (abstr.).
- Irving A. J., Bunch T. F., Kuehner S. M., Korotev R. L. and Classen N. C. (2008) Unique ultramafic shergottite Northwest Africa 4797: a highly shocked Martian wehrlite cumulate related to enriched basaltic (not “Iherzolitic”) shergottites. *Lunar Planet. Sci. XXXIX*. Lunar Planet. Inst., Houston. #2047 (abstr.).
- Jakosky B. M., Pepin R. O., Johnson R. O. and Fox J. L. (1994) Mars atmospheric loss and isotopic fractionation by solar-wind-induced sputtering and photochemical escape. *Icarus* **11**, 271–281.
- Jones J. H. (1986) A discussion of isotopic systematics and mineral zoning in the shergottites: evidence for a 180 m.y. igneous crystallization age. *Geochim. Cosmochim. Acta* **50**, 969–977.
- Jones J. H. (1989) Isotopic relationships among the shergottites, the nakhlites, and Chassigny. *Proc. Lunar Planet. Conf.* **19**, 465–474.
- Lanagan P. and McEwen A. (2003) Cerberus plains volcanism: constraints on temporal emplacement of the youngest lavas on Mars. *Sixth International Conference on Mars*. #3215 (abstr.).
- Laul J. C., Smith M. R., Wänke H., Jagoutz E., Dreibus G., Palme H., Spettel B., Burghele A., Lipschutz M. E. and Verkouteren R. M. (1986) Chemical systematics of the Shergotty meteorite and the composition of its parent body (Mars). *Geochim. Cosmochim. Acta* **50**, 909–926.
- Le Maitre R. W., Streckeisen A., Zanettin B., Le Bas M. J., Bonin B., Bateman P., Bellieni G., Dudek A., Efremova S., Keller J., Lameyre J., Sabine P. A., Schmid R., Sørensen H. and Woolley A. R. (2002) *Igneous Rocks: A Classification and Glossary of Terms* (ed. R. W. Le Maitre), second ed. Cambridge University Press, Cambridge.

- Leya I., Lange H.-J., Neumann S., Wieler R. and Michel R. (2000) The production of cosmogenic nuclides in stony meteoroids by galactic cosmic-ray particles. *Meteorit. Planet. Sci.* **35**, 259–286.
- Lindsley D. H., Papike J. J. and Bence A. E. (1972) Pyroxferroite: Breakdown at low pressure and high temperature. *Lunar Sci. III*. Lunar Planet. Inst., Houston. #483–485 (abstr.).
- Longhi J. (1991) Complex magmatic processes on Mars: inferences from the SNC meteorites. *Proc. Lunar Planet. Sci.* **21**, 695–709.
- Lorand J.-P., Chevrier V. and Sautter V. (2005) Sulfide mineralogy and redox conditions in some shergottites. *Meteorit. Planet. Sci.* **40**, 1257–1272.
- Mathew K. J. and Marti K. (2001) Early evolution of Martian volatiles: nitrogen and noble gas components in ALH84001 and Chassigny. *J. Geophys. Res.* **106**, 1401–1422.
- Mathew K. J., Marty B., Marti K. and Zimmermann L. (2003) Volatiles (nitrogen, noble gases) in recently discovered SNC meteorites, extinct radioactivities and evolution. *Earth Planet. Sci. Lett.* **214**, 27–42.
- Marti K., Kim J. S., Thakur A. N., McCoy T. J. and Keil K. (1995) Signatures of the Martian atmosphere in glass of the Zagami meteorite. *Science* **267**, 1981–1984.
- McEwen A. S., Preblich B. S., Turtle E. P., Artemieva N. A., Golombek M. P., Hurst M., Kirk R. L., Burr D. M. and Christensen P. R. (2005) The rayed crater Zunil and interpretations of small impact craters on Mars. *Icarus* **176**, 351–381.
- Misawa K. and Yamaguchi A. (2007) U–Pb Ages of NWA 856 Baddeleyite. *Meteorit. Planet. Sci.* **42**, A108. #5228 (abstr.).
- Misawa K., Yamada K., Nakamura N., Morikawa N., Yamashita K. and Premo W. (2006) Sm–Nd isotopic systematics of the lherzolitic shergottite Yamato-793605. *Antarct. Meteorit. Res.* **19**, 45–57.
- Morikawa N., Misawa K., Kondorosi G., Premo W. R., Tatsumoto M. and Nakamura N. (2001) Rb–Sr isotopic systematics of lherzolitic shergottite Yamato-793605. *Antarct. Meteorit. Res.* **14**, 47–60.
- Nishiizumi K. and Caffee M. W. (2006) Constraining the number of Lunar and Martian meteorite falls. *Meteorit. Planet. Sci.* **69**, A133 (abstr.).
- Nishiizumi K., Hillegonds D. J., McHargue L. R. and Jull A. J. T. (2004) Exposure and terrestrial histories of new lunar and Martian meteorites. *Lunar Planet. Sci. XXXV*. Lunar Planet. Inst., Houston. #1130 (abstr.).
- Neukum G., Ivanov B. A. and Hartmann W. K. (2001) Cratering records in the inner solar system in relation to the lunar reference system. *Space Sci. Rev.* **96**, 55–86.
- Neukum G., Jaumann R., Hoffmann H., Hauber E., Head J. W., Basilevsky A. T., Ivanov B. A., Werner S. C., van Gasselt S., Murray J. B. and McCord T. The HRSC Co-Investigator Team (2004) Recent and episodic volcanic and glacial activity on Mars revealed by the high resolution stereo camera. *Nature* **432**, 971–979.
- Neukum G., Basilevsky A. T., M. Chapman G., Werner S. C., van Gasselt S., Jaumann R., Hauber E., Hoffmann H., Wolf U., Head J. W., Greeley R. and McCord T. B., The HRSC Co-Investigator Team. (2007) Episodicity in the geological evolution of Mars: resurfacing events and ages from cratering analysis of image data and correlation with radiometric ages of Martian meteorites. *Lunar Planet. Sci. XXXVI*. Lunar Planet. Inst., Houston. #2271 (abstr.).
- Nyquist L. E., Wooden J., Bansal B., Wiesmann H., McKay G. and Bogard D. D. (1979) Rb–Sr age of the Shergotty achondrite and implications for metamorphic resetting of isochron ages. *Geochim. Cosmochim. Acta* **43**, 1057–1074.
- Nyquist L. E., Bogard D. D., Wiesmann H., Bansal B. M., Shih C.-Y. and Morris R. M. (1990) Age of a eucrite clast from the Bholghati howardite. *Geochim. Cosmochim. Acta* **54**, 2197–2206.
- Nyquist L. E., Bansal B., Wiesmann H. and Shih C.-Y. (1994) Neodymium, strontium, and chromium isotopic studies of the LEW86010 and Angra dos Reis meteorites and the chronology of the angrite parent body. *Meteorit. Planet. Sci.* **29**, 872–885.
- Nyquist L. E., Bansal B. M., Wiesmann H. and Shih C.-Y. (1995) “Martians” young and old: Zagami and ALH84001. *Proc. Lunar Planet. Sci.* **26**, 1065–1066.
- Nyquist L. E., Borg L. E. and Shih C.-Y. (1998) The shergottite age paradox and the relative probabilities for Martian meteorites of differing ages. *J. Geophys. Res.* **103**, 31445–31455.
- Nyquist L. E., Reese Y. D., Wiesmann H., Shih C.-Y. and Schwandt C. (2000) Rubidium–strontium age of the Los Angeles Shergottite (abstr.). *Meteorit. Planet. Sci.* **35**, A121–122.
- Nyquist L. E., Bogard D. D., Shih C.-Y., Greshake A., Stöffler D. and Eugster O. (2001a) Ages and geologic histories of Martian meteorites. *Space Sci. Rev.* **96**, 105–164.
- Nyquist L. E., Reese Y., Wiesmann H. and Shih C.-Y. (2001b) Age of EET79001B and implications for shergottite origins. *Lunar Planet. Sci. XXXII*. Lunar Planet. Inst., Houston. #1407 (abstr.).
- Nyquist L. E., Bogard D. D. and Shih C.-Y. (2001c) Radiometric chronology of the Moon and Mars. In *The Century of Space Science*, vol. II (eds. Bleeker, Geiss and Huber). Kluwer Academic Publishers, The Netherlands, pp. 1325–1376 (Chapter 55).
- Nyquist L. E., Shih C.-Y., Reese Y. D. and Irving A. J. (2004) Crystallization age of NWA 1460: Paradox revisited. *Second Conf. Early Mars*, Abstract #8041.
- Ott U. (1988) Noble gases in SNC meteorites: Shergotty, Nakhla, and Chassigny. *Geochim. Cosmochim. Acta* **52**, 1937–1948.
- Owen T. (1976) Volatile inventories on Mars. *Icarus* **28**, 171–177.
- Park J. (2005) Noble gas study of Martian meteorites: New insights on Mars. Ph.D. thesis. University of Tokyo.
- Park J. and Nagao K. (2003) Noble gas studies of Dhofar 378 Martian meteorite. *Meteorit. Planet. Sci.* **38**, A79 (abstr.).
- Park J., Bogard D. D., Mikouchi T. and McKay G. A. (2008) Dhofar 378 Martian shergottite: evidence of early shock melting. *J. Geophys. Res.* **113**, E08007.
- Pepin R. O. (1991) On the early evolution of terrestrial planet atmospheres and meteoritic volatiles. *Icarus* **92**, 2–79.
- Pepin R. O. and Carr M. H. (1992) Major issues and outstanding questions. In *Mars* (eds. H. Kieffer, B. Jakosky, C. Snyder and M. Mathews). Univ. Arizona Press, pp. 120–146.
- Phillips R. J., Zuber M. T., Solomon S. C., Golombek M. P., Jakosky B. M., Banerdt W. B., Smith D. E., Williams R. M. E., Hynek b. M., Aharonson O. and Hauck, II, S. A. (2001) Ancient geodynamics and global-scale hydrology on Mars. *Science* **291**, 2587–2591.
- Podosek F. A. and Brannon J. C. (1991) Chondrite chronology by initial $^{87}\text{Sr}/^{86}\text{Sr}$ in phosphates? *Meteoritics* **26**, 145–152.
- Popova O. P., Hartmann W. K., Nemtchinov I. V., Richardson D. C. and Berman D. C. (2007) Crater clusters on Mars: shedding light on Martian ejecta launch conditions. *Icarus* **190**, 50–73.
- Rotenberg E. and Amelin Y. (2001) Combined initial Sr, Sm–Nd and U–Pb systematics of chondritic phosphates: how reliable are the ages? *Lunar Planet. Sci. XXXII*. Lunar Planet. Inst., Houston. #1675 (abstr.).
- Rotenberg E. and Amelin Y. (2002) Rb–Sr chronology of chondrules from ordinary chondrites. *Lunar Planet. Sci. XXXIII*. Lunar Planet. Inst., Houston. #1605 (abstr.).
- Rumble, III, D. and Irving A. J. (2009) Dispersion of oxygen isotopic compositions among 42 Martian meteorites determined by laser fluorination: evidence for assimilation of (ancient)

- altered crust. *Lunar Planet. Sci. XV*. Lunar Planet. Inst., Houston. #2293 (abstr.).
- Ryder G., Bogard D. and Garrison D. (1991) Probable age of Autolycus and calibration of lunar stratigraphy. *Geology* **19**, 143–146.
- Schwenzer S. P., Herrmann S., Mohapatra R. K. and Ott U. (2007) Noble gases in mineral separates from three shergottites: Shergotty, Zagami, and EETA79001. *Meteorit. Planet. Sci.* **42**, 387–412.
- Shih C.-Y., Nyquist L. E., Bogard D. D., McKay G. A., Wooden J. L., Bansal B. M. and Wiesmann H. (1982) Chronology and petrogenesis of young achondrites, Shergotty, Zagami, and ALHA77005: late magmatism on a geologically active planet. *Geochim. Cosmochim. Acta* **46**, 2323–2344.
- Shih C.-Y., Nyquist L. E. and Wiesmann H. (1999) Samarium–neodymium and rubidium–strontium systematics of nakhlite Governador Valadares. *Meteorit. Planet. Sci.* **34**, 647–655.
- Shih C.-Y., Nyquist L. E., Wiesmann H., Reese Y. and Misawa K. (2005) Rb–Sr and Sm–Nd dating of olivine-phyric shergottite Yamato 980459: petrogenesis of depleted shergottites. *Antarct. Meteorit. Res.* **18**, 46–65.
- Shih C.-Y., Nyquist L. E. and Reese Y. (2006) Rb–Sr and Sm–Nd isotopic studies of Antarctic nakhlite MIL03346. *Lunar Planet. Sci. XXXVII*. Lunar Planet. Inst., Houston #1701 (abstr.).
- Shih C.-Y., Nyquist L. E. and Reese Y. (2007) Rb–Sr and Sm–Nd isotopic studies of Martian depleted shergottites SaU094/005. *Lunar Planet. Sci. XXXVIII*. Lunar Planet. Inst., Houston. #1745 (abstr.).
- Steiger R. H. and Jäger E. (1977) Subcommittee on geochronology: convention on the use of decay constants in geo- and cosmochronology. *Earth Planet. Sci. Lett.* **36**, 359–362.
- Stöffler D. and Ryder G. (2001) Stratigraphy and isotope ages of lunar geologic units: chronological standard for the inner solar system. *Space Sci. Rev.* **96**, 9–54.
- Stolper E. M. and McSween H. Y. (1979) Petrology and origin of the shergottite meteorites. *Geochim. Cosmochim. Acta* **43**, 1475–1498.
- Symes S. J. K., Borg L. E., Shearer C. K. and Irving A. J. (2008) The age of the Martian meteorite Northwest Africa 1195 and the differentiation history of the shergottites. *Geochim. Cosmochim. Acta* **72**, 1696–1710.
- Tanaka K. L. (1986) The stratigraphy of Mars. *Proc. Lunar Planet. Sci.* **17**, Part 1. *J. Geophys. Res.* **91**, Suppl., E139–E158.
- Tanaka K. L., Scott D. H. and Greeley, R. (1992) In *Mars* (eds. H. H. Kieffer, B. M. Jakosky, C.W. Snyder and M. S. Matthews). The University of Arizona Press, Tucson. pp. 345–382.
- Tanaka, K. L., Skinner, Jr., J. A. and Hare, T. M. (2005) Geologic map of the northern plains region of Mars. *U.S. Geol. Surv. Sci. Invest. Map SIM-2888*, scale 1:15,000,000.
- Taylor G. J., Stopar J. D., Boynton W. V., Karuntillake S., Keller J. M., Brückner J., Wänke H., Dreibus G., Kerry K. E., Reedy R. C., Evans L. G., Starr R. D., Martel M. V., Squyres S. W., Gasnault O., Maurice S., d’Uston C., Englert P., Dohm J. M., Baker V. R., Hamara D., Janes D., Sprague A. L., Kim K. J., Drake D. M., McLennan S. M. and Hahn B. C. (2007) Variations in K/Th on Mars. *J. Geophys. Res.* **101**, E03S06. [10.1029/2006JE002676](https://doi.org/10.1029/2006JE002676), 2006.
- Taylor L. A. and Misra K. C. (1975) Mineralogy and petrology of Apollo 15 rock 15075. *Lunar Sci. VI*. Lunar Planet. Inst., Houston. #801–803. (abstr.).
- Terribilini D., Eugster O., Burger M., Jakob A. and Krähenbühl U. (1998) Noble gases and chemical composition of Shergotty mineral fractions, Chassigny, and Yamato 793605: the trapped argon-40/argon-39 ratio and ejection times of Martian meteorites. *Meteorit. Planet. Sci.* **33**, 677–684.
- Treiman A. H. (1995) S ≠ NC: multiple source areas for Martian meteorites. *J. Geophys. Res.* **100**, 5329–5340.
- Treiman A. H., Dyar M. D., McCanta M., Noble S. K. and Pieters C. M. (2007) Martian dunite NWA 2737: petrographic constraints on geological history, shock events, and olivine color. *J. Geophys. Res.* **112**, E04002. doi:10.1029/2006JE002777.
- Wadhwa M., McSween H. Y. and Crozaz G. (1994) Petrogenesis of shergottite meteorites inferred from minor and trace element microdistributions. *Geochim. Cosmochim. Acta* **58**, 4213–4229.
- Walton E. L., Kelly S. P. and Spray J. G. (2007) Shock implantation of Martian atmospheric argon in four basaltic shergottites: a laser probe Ar/Ar investigation. *Geochim. Cosmochim. Acta* **71**, 497–520.
- Ware N. G. and Lovering J. F. (1970) Electron microprobe analyses of phases in lunar samples. *Science* **167**, 517–520.
- Warren P. H. (1994) Lunar and Martian meteorite delivery services. *Icarus* **111**, 338–363.
- Warren P. H. and Kallemeyn G. W. (1997) Yamato-793605, EET79001 and other presumed Martian meteorites: compositional clues to their origins. *Antarct. Meteorit. Res.* **10**, 61–81.
- Warren P. H., Greenwood J. P. and Rubin A. E. (2004) Los Angeles: a tale of two stones. *Meteorit. Planet. Sci.* **39**, 137–156.
- Wasserburg G. J., Jacobsen S. B., DePaolo D. J., McCulloch M. T. and Wen T. (1981) Precise determination of Sm/Nd ratios, Sm and Nd isotopic abundances in standard solutions. *Geochim. Cosmochim. Acta* **45**, 2311–2323.
- Werner S. C. (2005) Major Aspects of the Chronostratigraphy and Geologic Evolutionary History of Mars. Ph.D. thesis. Freie Universitaet Berlin, Cuvillier Verlag, Goettingen.
- Wiens R. C., Becker R. H. and Pepin R. O. (1986) The case for Martian origin of the shergottites. II. Trapped and indigenous gas components in EETA 79001 glass. *Earth Planet. Sci. Lett.* **77**, 149–158.
- Wiens R. C. and Pepin R. O. (1988) Laboratory shock emplacement of noble gases, nitrogen, and carbon dioxide into basalt, and implications for trapped gases in shergottite EETA79001. *Geochim. Cosmochim. Acta* **52**, 295–307.
- Williamson J. H. (1968) Least-squared fitting of a straight line. *Can. J. Phys.* **46**, 1845–1847.
- Wooden J. L., Shih C.-Y., Nyquist L. E., Bansal B. M., Wiesmann H. and McKay G. A. (1982) Rb–Sr and Sm–Nd isotopic constraints on the origin of EETA79001: a second Antarctic shergottite. *Lunar Planet. Sci. XIII*, Lunar Planet. Inst., Houston. #879–880 (abstr.).

Associate editor: Gregory F. Herzog